Multi-Regge factorization in inclusive two-particle production

Michael J. Puhala

Department of Physics, University of Illinois at Urbana-Champaign, Urbana, Illinois 61801
(Received 14 May 1979)

We consider in detail the multi-Regge expansion for the eight-particle amplitude with one triple-Regge and two double-Regge couplings. We show that under trivial conditions and with a suitable choice of helicity contours, the double-Regge couplings in the multi-Regge (MR) limit are identical, to leading order, with couplings obtained in the mixed helicity-pole–Regge-pole (HPRP) limit appropriate to inclusive reactions. Since we do not need to introduce any dependences on any additional variables, our conditions are somewhat simpler than the results of others. As a plausibility argument for the identity of the MR and HPRP limit, we present an intuitive picture of how helicity poles may be visualized at the triple-Regge vertex. Assuming the mentioned identity, we calculate the diffractive contribution to $\pi^- p \to \rho^0 \pi^- X$ and discuss the problem of isolating this mechanism experimentally. We propose experimental tests for the identity of the couplings and relate this to the problem of observing the A_1.

I. INTRODUCTION

In a previous paper,[1] we developed a Reggeized Deck model satisfying the Steinmann relation for the exclusive reaction $\pi^- p \to \rho^0 \pi^- p$. Owing to the separation of the normal threshold singularities in the $\rho^0 \pi^-$ and the $\pi^- p$ channels, we found that we could interpret the two resulting terms as being either resonant or nonresonant in the $\rho^0 \pi^-$ channel. We showed that an A_1 resonance, if present in the data, would be obscured both in magnitude and in phase by the nonresonant piece. One wonders whether such effects might be minimized in other reactions; an interesting candidate is the reaction

$$\pi^- p \to \rho^0 \pi^- X$$
$$\searrow \pi^- \pi^+ \tag{1.1}$$
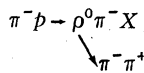
shown in Fig. 1. If one uses the Mueller optical theorem,[2,3] one can write the inclusive two-particle distribution for this reaction as the discontinuity of a $4 \to 4$ amplitude. Since we have determined the double-Regge couplings that describe the exclusive reaction, and since triple-Regge couplings have been determined from data on $pp \to pX$, one expects that these results can be combined using the multi-Regge formalism to yield information about (1.1).

As we will show, certain complications arise. In particular, if we attempt a "multi-Regge" expansion of the $4 \to 4$ amplitude, we obtain a familiar result, namely that the amplitude is dominated by both Regge poles and helicity poles.[3-6] In the past, others have investigated this problem,[10] and have determined that the double-Regge couplings in the multi-Regge limit and the mixed helicity-pole–Regge-pole (HPRP) limit are different, un-

less the Regge residues obey certain relations. In this paper, we will show that by a suitable choice of helicity contour, the conditions that produce identical couplings in the two limits become quite simple; in fact, we will show that it is not necessary to introduce any new dependences on any new variables in order to achieve this identity. We develop an intuitive picture of the HPRP limit to show that this identity is in fact an elegant result. We propose some experimental tests to check this result, and perform some rough calculations assuming its validity.

In Sec. II, we review some basics of inclusive cross sections, and express the ρ-π mass spectrum in terms of the discontinuity of an eight-particle amplitude M_8. In addition, we will discuss the legitimacy of using a multi-Regge expansion for this process.

In Sec. III, we write an $SO(2,1)$ expansion for M_8, and relate the invariant subenergies of the external particles to the $SO(2,1)$ parameters in the multi-Regge and HPRP limits. We establish a correspondence between the $SO(2,1)$ parameters for M_8 in the kinematic limit appropriate to the inclusive cross section, and a parametrization of a "naive" set of momenta, treating the momentum of the unobserved particles Q_X as that of a quasiparticle.

In Sec. IV, we analytically continue the $SO(2,1)$ parameters into an ordinary $O(3)$ parametrization, and write down the resulting partial-wave expansion for M_8. This determines the analytic continuation of M_8 that yields the inclusive cross section. There are two types of angle parameters that result from this continuation process. There are polar angles, which specify the angle between two three-vectors in a particular rest frame. In addition, 'here are azimuthal angles which specify
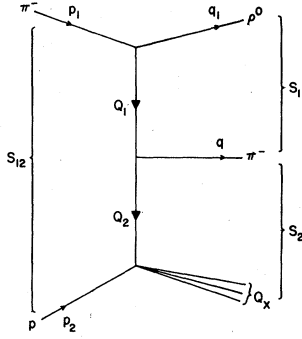

FIG. 1. Kinematics for the inclusive reaction $\pi^- p \to \rho^0 \pi^- X$.

the orientations between planes formed by sets of three-momentum vectors in certain rest frames. We study the behavior of the O(3) parameters in various asymptotic limits, and show in detail that in the multi-Regge limit, a set of polar angles becomes large, but in the HPRP limit, a set of polar and azimuthal angles becomes large.

In Sec. V, we show that with a suitable choice of helicity contours, the multi-Regge and the HPRP expansions agree if certain simple conditions are satisfied.

In Sec. VI, we develop an intuitive picture of the HPRP limit. We show how it contributes to the inclusive cross section, and relate the identity of the couplings to the commutativity of the asymptotic limits.

In Sec. VII, we assume the identity of the couplings in the multi-Regge and HPRP limits, and determine the remaining residues by unitarity. We isolate the HRPR limit through the use of kinematic cuts, and show that these cuts effectively isolate "diffractively" produced $\rho\pi$ systems. We extend our result to $\pi^- p \to \pi^- \pi^+ \pi^- X$ and suggest an experimental test for the identity of the couplings in the multi-Regge and HPRP limit. We compare with reported data.

In Sec. VIII, we relate our results to the problem of observing the A_1, and suggest mechanism by which it might be seen.

In Sec. IX, we summarize the main results of this analysis.

The reader who is concerned only with the phenomenological aspects of this analysis may wish to skip sections III, IV, V, and VI altogether. Those who are more theoretically inclined may find it useful to skip Sec. V on the first reading, in order to follow the "geometric" arguments used to characterize the helicity poles at the triple-Regge vertex.

II. MUELLER ANALYSIS

In Fig. 1, we display the kinematics for the reaction $\pi^- p \to \rho^0 \pi^- X$, where X stands for the unobserved particles in the final state. The momenta p_1 and p_2 are those of the incident pion and proton, respectively; q_1 and q are the momenta of the outgoing ρ and pion. The missing four-momentum is Q_X, and the missing mass is M_X. The important kinematic invariants are given by

$$s_{12} = (p_1 + p_2)^2, \quad s_1 = (q_1 + q)^2, \quad s_2 = (p_1 + p_2 - q_1)^2, \quad s_X = (p_1 + p_2 - q_1 - q)^2 = Q_X^2,$$

$$t_1 = (p_1 - q_1)^2, \quad t_2 = (p_2 - Q_X)^2, \quad M_{\rho\pi} = \sqrt{s_1}, \quad M_X = \sqrt{s_X}. \tag{2.1}$$

In order to write a general expression for the ρ-π mass spectrum, we first consider the amplitude for $\pi^- p \to (n+1)\,\rho^0\text{'s} + (m+1)\,\pi^-\text{'s} + X'$, where the unobserved state X' contains no particles which are either ρ^0's or π^-'s (see Fig. 2). If we label the momenta of the ρ^0's by $k_0, k_1, \ldots, k_n$, with $k_0 = q_1$, and label the momenta of the π^-'s by $l_0, l_1, \ldots, l_m$, with $l_0 = q$, we may treat all particles as being spinless, and write the differential cross section for this reaction as[2]

$$\frac{d\sigma}{dq_1 dq\, dk_1 \cdots dk_n dl_1 \cdots dl_n} = \frac{(2\pi)^4}{2\lambda^{1/2}(s_{12}, m^2, m_N^2)} \sum_{X'} \frac{1}{F_{X'}} \int \prod_{r=1}^{s(X')} \frac{d^3 p_{x_r}}{(2\pi)^3 2(p_{x_r})_0}$$

$$\times \delta^4\!\left(p_1 + p_2 - q_1 - q - \sum_{i=1}^{n} k_i - \sum_{j=1}^{m} l_j - \sum_{r=1}^{s(X')} p_{x_r}\right)$$

$$\times |\langle q_1, q; k_i; l_j; p_{x_r} |M| p_1, p_2\rangle|^2, \tag{2.2}$$

where $\lambda(a, b, c) = a^2 + b^2 + c^2 - 2ab - 2ac - 2bc$. In the above, the phase-space element is given by $dk_i = d^3 k_i / (2\pi)^3 2(k_i)_0$ and $F_{X'}$ is the appropriate statistical factor for the unobserved state X', which contains $s(X')$ unobserved particles. The inclusive ρ-π distribution is given by

$$\frac{d\sigma}{dq_1 dq} = \sum_{n,m=0}^{\infty} \frac{1}{n!\,m!} \int \prod_{i=1}^{n} \frac{d^3 k_i}{(2\pi)^3 2k_{i_0}} \prod_{j=1}^{m} \frac{d^3 l_j}{(2\pi)^3 2 l_{j_0}} \frac{d\sigma}{dq_1 dq\, dk_1 \cdots dk_n dk_n dl_1 \cdots dl_m}. \tag{2.3}$$
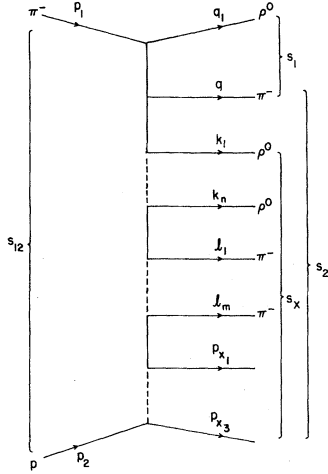
FIG. 2. A particular final state containing $(n+1)$ ρ^0's, $(l+1)$ π^-'s, and x_s particles of other types.

Let us now attempt to write the ρ-π mass spectrum in terms of $d\sigma/dq_1 dq$. It is convenient to consider vectors in the ρ-π rest frame and the M frame; we denote four-vectors in the M frame by a superscript M. In Fig. 3, we see that the M frame is defined by the condition $\vec{q}_1^M + \vec{q}^M = 0$ and the orientations

$$p_1^M = (p_{10}^M, 0, 0, |\vec{p}_1^M|),$$

$$q_1^M = (q_{10}^M, |\vec{q}_1^M|\sin\theta_1\cos\phi_1, |\vec{q}_1^M|\sin\theta_1\sin\phi_1, |\vec{q}_1^M|\cos\theta_1),$$

$$(2.4)$$

$$Q_X^M = (Q_{X_0}^M, |\vec{Q}_X^M|\sin\psi_2, 0, |\vec{Q}_X^M|\cos\psi_2).$$

The M-frame quantities are related to the invari-

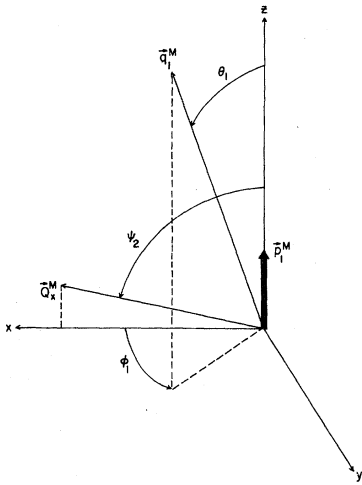FIG. 3. Orientation of vectors in the M frame (ρ-π rest frame).

ants in Eq. (2.1) by the following expressions:

$$p_{10}^M = \frac{s_1 + m_\pi^2 - t_2}{2\sqrt{s_1}}, \quad |\vec{p}_1^M| = \frac{\lambda^{1/2}(s_1, m_\pi^2, t_2)}{2\sqrt{s_1}},$$

$$Q_{10}^M = \frac{s_{12} - s_1 - s_X}{2\sqrt{s_1}}, \quad |\vec{Q}_X^M| = \frac{\lambda^{1/2}(s_{12}, s_1, s_X)}{2\sqrt{s_1}},$$

$$q_{10}^M = \frac{s_1 + m_\rho^2 - m_\pi^2}{2\sqrt{s_1}}, \quad |\vec{q}_1^M| = \frac{\lambda^{1/2}(s_1, m_\rho^2, m_\pi^2)}{2\sqrt{s_1}},$$

$$q_0^M = \frac{s_1 + m_\pi^2 - m_\rho^2}{2\sqrt{s_1}},$$

$$(2.5)$$

$$\cos\theta_1 = \frac{t_1 + 2p_{10}^M q_{10}^M - m_\pi^2 - m_\rho^2}{2|\vec{p}_1^M||\vec{q}_1^M|},$$

$$\sin\theta_1 = (1 - \cos^2\theta_1)^{1/2},$$

$$\cos\psi_2 = \frac{2p_{10}^M Q_{X0}^M + s_1 + m_N^2 - t_2 - s_{12}}{2|\vec{p}_1^M||\vec{Q}_X^M|},$$

$$\sin\psi_2 = (1 - \cos^2\psi_2)^{1/2}.$$

The inclusive ρ-π mass spectrum is then given by

$$\frac{d\sigma}{dM_{\rho\pi}} = \frac{1}{2^4(2\pi)^5\lambda^{1/2}(s_{12}, m_\pi^2, m_N^2)}$$

$$\times \int ds_X \int dt_2 \int dt_1 \int \frac{d\phi_1}{|\vec{p}_1^M|} \frac{d\sigma}{dq_1 dq}. \quad (2.6)$$

We observe from Eqs. (2.2) and (2.3) that the term in Eq. (2.2) with $n = m = 0$ will yield a δ-function contribution to the s_X integral at $s_X = m_N^2$. This contribution, due to the "elastic" $\rho^0\pi^-p$, can cause problems in the presence of poor missing-mass resolution. This problem will be discussed in Sec. VII.

By Mueller's optical theorem,[3,4] $d\sigma/dq_1 dq$ may be written in terms of the discontinuity in s_X of the $4 \to 4$ amplitude shown in Fig. 4:

$$\frac{d\sigma}{dq_1 dq} = \frac{1}{2i\lambda^{1/2}(s_{12}, m_\pi^2, m_N^2)} \mathrm{Disc}_{s_X} M_8(\mathrm{MFD}). \quad (2.7)$$

The expression $M_8(\mathrm{MFD})$ denotes the eight-particle amplitude evaluated in the "Mueller forward direction" denoted by the limit

$$p_1 = p_1' \quad p_2 = p_2' \quad q_1 = q_1' \quad q = q'. \quad (2.8)$$

It is our aim to see whether or not the Deck-type bump is predicted for the ρ-π mass spectrum. Our prediction will be based upon a multi-Regge
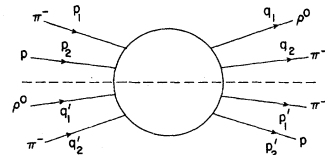

FIG. 4. General $4 \to 4$ amplitude. Arrows pointing inward denote incoming particles, etc. Dashed line denotes discontinuity in missing mass squared.
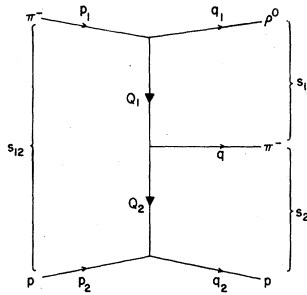
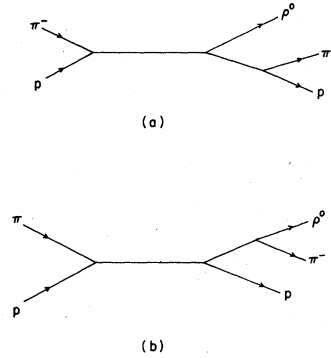FIG. 5. Kinematics for the exclusive reaction $\pi^- p \to \rho^0 \pi^- p$.

(a)

(b)

FIG. 6. Normal threshold structure of the five-particle amplitude $M_5 = H_1 + H_2$. (a) H_1, with $\lambda = \alpha_1 - n$, $n = 0, 1, 2, \ldots$. (b) H_2, with $\lambda = \alpha_2 - n$.

expansion of the eight-particle amplitude in Eq. (2.7). Owing to the relatively low value of $M_{\rho\pi}$ in this region (< 1.5 GeV), some comments on the plausibility of this procedure are in order.

For the exclusive reaction $\pi^- p \to \rho^0 \pi^- p$ (see Fig. 5), the kinematic region of interest is given by

$$t_1, t_2, s_1 \text{ fixed}, \quad s_{12}, s_2 \to \infty . \tag{2.9}$$

We will refer to the above as the A_1 region. In Ref. 1, the exclusive reaction was described by a double-Regge amplitude appropriate to the kinematic region

$$t_1, t_2, \eta_{12} = s_{12}/s_1 s_2 \text{ fixed}, \quad s_1, s_2, s_{12} \to \infty , \tag{2.10}$$

which we shall term the double-Regge region.[4] From Ref. 1, the five-particle amplitude can be written $M_5 = H_1 + H_2$, where

$$H_1 = \beta_1(t_1)\beta_2(t_2)\Gamma(-\alpha_1)\Gamma(-\alpha_2)$$
$$\times s_2^{\alpha_2 - \alpha_1} s_{12}^{\alpha_1} \xi_1 \xi_{21} V_1(t_1, t_2; \eta_{12}) , \tag{2.11}$$

$$H_2 = \beta_1(t_1)\beta_2(t_2)\Gamma(-\alpha_1)\Gamma(-\alpha_2)$$
$$\times s_1^{\alpha_1 - \alpha_2} s_{12}^{\alpha_2} \xi_2 \xi_{12} V_2(t_1, t_2; \eta_{12}) . \tag{2.12}$$

The "reduced" contributions to the pion–Pomeron–Reggerized-pion vertex are given by

$$V_1(t_1, t_2; \eta_{12}) = \frac{P(t_1, t_2)\Gamma(\alpha_1 - \alpha_2)}{M(t_1, t_2)^{\alpha_1}\Gamma(-\alpha_2)\Gamma(1 + \alpha_1)}$$
$$\times \left[F\left(-\alpha_1, -\alpha_1 | 1 - \alpha_1 + \alpha_2 | \frac{M}{\eta_{12}}\right) \right.$$
$$\left. - \alpha_1 F\left(1 - \alpha_1, -\alpha_1 | 1 - \alpha_1 + \alpha_2 | \frac{M}{\eta_{12}}\right) \right] , \tag{2.13}$$

$$V_2(t_1, t_2; \eta_{12}) = \frac{P(t_1, t_2)\Gamma(\alpha_2 - \alpha_1)}{M(t_1, t_2)^{\alpha_2}\Gamma(-\alpha_1)\Gamma(1 + \alpha_2)}$$
$$\times \left[F\left(-\alpha_2, -\alpha_2 | 1 + \alpha_1 - \alpha_2 | \frac{M}{\eta_{12}}\right) \right.$$
$$\left. - \alpha_2 F\left(1 - \alpha_2, -\alpha_2 | 1 - \alpha_1 + \alpha_2 | \frac{M}{\eta_{12}}\right) \right] . \tag{2.14}$$

Quantities appearing in the last two equations were defined in Ref. 1.

The legitimacy of applying the double-Regge formula to the region (2.10) may be readily appreciated if we examine the singularity structure of Eqs. (2.11) and (2.12). In the physical region of the exclusive reaction, V_1 and V_2 are free of cuts in η_{12}. If we let λ be the complex helicity of the exchanged Reggeons, the term H_1 is due to the contributions from helicity poles at $\lambda = \alpha_1 - n$, where α_1 is the pion trajectory appearing in the t_1 channel, and $n = 0, 1, 2, \ldots$; similarly, H_2 is due to contributions from helicity poles at $\lambda = \alpha_2 - n$, where α_2 is the Pomeron trajectory appearing in the t_2 channel.[4,5] Since V_1 and V_2 are free of cuts in η_{12}, H_1 has cuts in s_2 and s_{12}, and thus a discontinuity structure appropriate to the tree graph of Fig. 6(a); similarly, H_2 has cuts in s_1 and s_{12}, and a discontinuity structure corresponding to Fig. 6(b).

If we extrapolate the amplitude A_5 in the variable s_1 from the double-Regge region down into the A_1 region, the term H_1 dominates the term H_2. Since s_2 and s_{12} remain large in the A_1 region, the term H_1 is expected to have the correct phase and power-law behavior, since it contains the normal threshold singularities in these channels. On the other hand, the term H_2, which contains the normal threshold singularities in the s_1 and s_{12} channels, can at best be expected to approximate the average behavior of the amplitude in s_1 in a "dual" sense, since $M_{\rho\pi}$ is close to threshold. This is sufficient to give excellent agreement with the data, however, since H_2 is much smaller than H_1.

We see then that it is consistent to regard the term H_2 as containing a dual average to resonances in the s_1 channel, and to apply our double-Regge formula in the A_1 region. It seems reasonable to expect that a multi-Regge analysis of the eight-

particle amplitude in Eq. (2.7) would have comparable success in describing inclusive A_1 production through a similar mechanism. Let us now attempt such an analysis.

III. THE SO (2,1) EXPANSION AND ASYMPTOTIC LIMITS

In this section, we will consider an SO(2, 1) parametrization of the eight-particle amplitude, symbolized by Fig. 7. Following a similar treatment of the six-particle amplitude by Abarbanel and Schwimmer,[6] we shall determine the asymptotic behavior of the subenergy invariants in terms of the group variables. In Sec. IV we will continue the SO(2, 1) expansion into an ordinary O(3) angular momentum expansion, and demonstrate the manner in which singularities in complex angular momenta and helicities determine the asymptotic behavior of the amplitude in the inclusive A_1 region.

In Fig. 7, we have taken

$$k_1 = p_1, \quad k_{1'} = q_1, \quad k_2 = Q_1,$$
$$k_{2'} = q, \quad k_3 = p_2, \quad k_{5'} = Q_4. \tag{3.1}$$

Using a technique due to Toller,[7] we can describe a general configuration of momenta by the action of the group SO(2, 1) acting on a set of standard reference momenta. We denote our reference momenta by $k_i^{s_i}$, where the superscript s_i denotes the frame in which $Q_i^{s_i} = [0, 0, 0, \sqrt{-t_i}]$ and $k_i^{s_i} = [(k_i^{s_i})_t, 0, 0, (k_i^{s_i})_z]$. The reference momenta, which depend only on the t_i's, are given in Table I. We define the reference frames $F_1, F_2, \ldots, F_5$ such that in the frame F_i, the momenta $k_i^{F_i}, k_{i'}^{F_i}$ are given by

$$k_i^{F_i} = g_i(\chi_i, \xi_i, \phi_i)k_i^{s_i},$$
$$k_{i'}^{F_i} = g_i(\chi_i, \xi_i, \phi_i)k_{i'}^{s_i}. \tag{3.2}$$

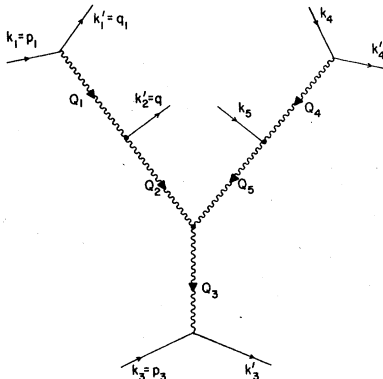The SO(2, 1) group elements $g_i(\chi_i, \xi_i, \phi_i)$ are given

FIG. 7. Tree diagram symbolizing SO(2, 1) parametrization of M_8.

TABLE I. Reference momenta for the SO(2, 1) parametrization $[x = (t, \vec{x})]$.

$$Q_i^{s_i} = (0, 0, 0, \sqrt{-t_i})$$

$$k_1^{s_1} = \left[\frac{\lambda^{1/2}(m_\rho^2, m_\pi^2, t_1)}{2\sqrt{-t_1}}, 0, 0, \frac{m_\rho^2 - m_\pi^2 - t_1}{2\sqrt{-t_1}} \right]$$

$$k_{1'}^{s_1} = \left[\frac{\lambda^{1/2}(m_\rho^2, m_\pi^2, t_1)}{2\sqrt{-t_1}}, 0, 0, \frac{t_1 + m_\rho^2 - m_\pi^2}{2\sqrt{-t_1}} \right]$$

$$k_2^{s_2} = \left[\frac{\lambda^{1/2}(m_\pi^2, t_1, t_2)}{2\sqrt{-t_2}}, 0, 0, \frac{m_\pi^2 - t_1 - t_2}{2\sqrt{-t_2}} \right]$$

$$k_{2'}^{s_2} = \left[\frac{\lambda^{1/2}(m_\pi^2, t_1, t_2)}{2\sqrt{-t_2}}, 0, 0, \frac{t_2 + m_\pi^2 - t_1}{2\sqrt{-t_2}} \right]$$

$$k_3^{s_3} = [(m_N^2 - \tfrac{1}{4}t_3)^{1/2}, 0, 0, -\tfrac{1}{2}\sqrt{-t_3}]$$

$$k_{3'}^{s_3} = [(m_N^2 - \tfrac{1}{4}t_3)^{1/2}, 0, 0, \tfrac{1}{2}\sqrt{-t_3}]$$

$$k_4^{s_4} = \left[\frac{\lambda^{1/2}(m_\pi^2, m_\rho^2, t_4)}{2\sqrt{-t_4}}, 0, 0, \frac{m_\pi^2 - m_\rho^2 - t_4}{2\sqrt{-t_4}} \right]$$

$$k_{4'}^{s_4} = \left[\frac{\lambda^{1/2}(m_\pi^2, m_\rho^2, t_4)}{2\sqrt{-t_4}}, 0, 0, \frac{t_4 + m_\pi^2 - m_\rho^2}{2\sqrt{-t_4}} \right]$$

$$k_5^{s_5} = \left[\frac{\lambda^{1/2}(m_\pi^2, t_4, t_5)}{2\sqrt{-t_5}}, 0, 0, \frac{t_4 - m_\pi^2 - t_5}{2\sqrt{-t_5}} \right]$$

$$k_{5'}^{s_5} = \left[\frac{\lambda^{1/2}(m_\pi^2, t_4, t_5)}{2\sqrt{-t_5}}, 0, 0, \frac{t_5 + t_4 - m_\pi^2}{2\sqrt{-t_5}} \right]$$

by

$$g_i(\chi_i, \xi_i, \phi_i) = B_y(\chi_i)B_x(\xi_i)R_z(\phi_i), \quad i = 2, 3, 5, \tag{3.3a}$$

$$g_i(\chi_i, \xi_i, \phi_i) = R_z(\chi_i)B_x(\xi_i)R_z(\phi_i), \quad i = 1, 4. \tag{3.3b}$$

In the above, B_y and B_x correspond to Lorentz boosts in the y and x directions; R_z corresponds to a rotation about the z axis. Their explicit matrix realizations are given by the well-known forms

$$B_x(\xi_i) = \begin{bmatrix} \cosh\xi_i & \sinh\xi_i & 0 & 0 \\ \sinh\xi_i & \cosh\xi_i & 0 & 0 \\ 0 & 0 & 1 & 0 \\ 0 & 0 & 0 & 1 \end{bmatrix},$$

$$B_y(\chi_i) = \begin{bmatrix} \cosh\chi_i & 0 & \sinh\chi_i & 0 \\ 0 & 1 & 0 & 0 \\ \sinh\chi_i & 0 & \cosh\chi_i & 0 \\ 0 & 0 & 0 & 1 \end{bmatrix}, \tag{3.4}$$

$$R_z(\chi_i) = \begin{bmatrix} 1 & 0 & 0 & 0 \\ 0 & \cos\chi_i & -\sin\chi_i & 0 \\ 0 & \sin\chi_i & \cos\chi_i & 0 \\ 0 & 0 & 0 & 1 \end{bmatrix}.$$

The motivation behind the choice of Eqs. (3.3a) and (3.3b) will become apparent in Sec. IV.

In order to apply our analysis to the amplitude in Eq. (2.7), we consider the case where all the Q_i are spacelike. It was shown by Misheloff[8] that the frame F_3 can be defined so that Q_2, Q_3, and Q_5 all lie in the x-z plane, and

$$Q_2^{F_3} = R_y(\theta_2) Q_2^{F_2} ,$$
$$Q_5^{F_3} = R_y(\theta_5) Q_5^{F_5} , \qquad (3.5)$$

where

$$\cos\theta_2 = \frac{t_5 - t_2 - t_3}{2\sqrt{-t_2}\sqrt{-t_3}}, \quad \sin\theta_2 = \frac{[-\lambda(t_2, t_3, t_5)]^{1/2}}{2\sqrt{-t_2}\sqrt{-t_3}} ,$$

$$\cos\theta_5 = \frac{t_2 - t_3 - t_5}{2\sqrt{-t_3}\sqrt{-t_5}}, \quad \sin\theta_5 = \frac{[-\lambda(t_2, t_3, t_5)]^{1/2}}{2\sqrt{-t_3}\sqrt{-t_5}} , \qquad (3.6)$$

$$R_y(\theta_i) = \begin{bmatrix} 1 & 0 & 0 & 0 \\ 0 & \cos\theta_i & 0 & \sin\theta_i \\ 0 & 0 & 1 & 0 \\ 0 & -\sin\theta_i & 0 & \cos\theta_i \end{bmatrix} .$$

We take Eq. (3.5) to be the general transformation between four-vectors in the frames F_2, F_3, and F_5.

The relations between frames F_1 and F_2 and between frames F_4 and F_5 have been discussed previously in terms of the Bali-Chew-Pignotti variables.[9] The frame F_1 is reached from the standard frame s_2 by boosting along the z axis, with a similar relation between frames s_5 and F_4. For any four-vector A, we have that

$$A^{s_2} = B_z(\kappa_{21}) A^{F_1} ,$$
$$A^{s_5} = B_z(\kappa_{54}) A^{F_4} , \qquad (3.7)$$

where

$$\cosh\kappa_{21} = \frac{m_\pi^2 - t_1 - t_2}{2\sqrt{-t_1}\sqrt{-t_2}}, \quad \sinh\kappa_{21} = \frac{\lambda^{1/2}(m_\pi^2, t_1, t_2)}{2\sqrt{-t_1}\sqrt{-t_2}} ,$$

$$\cosh\kappa_{54} = \frac{m_\pi^2 - t_4 - t_5}{2\sqrt{-t_4}\sqrt{-t_5}}, \quad \sinh\kappa_{54} = \frac{\lambda^{1/2}(m_\pi^2, t_4, t_5)}{2\sqrt{-t_4}\sqrt{-t_5}} . \qquad (3.8)$$

To illustrate the general procedure for specifying the momenta in a particular frame, we will write our expression for the four-vector k_1 in the F_3 frame. We see that Eq. (3.2) gives us k_1 in the F_1 frame, Eq. (3.7) gives us k_1 in the s_2 frame, Eq. (3.2) gives us k_1 in the F_2 frame, and Eq. (3.5) gives us k_1 in the F_3 frame. The net result is

$$k_1^{F_3} = R_y(\theta_2) g_2(\chi_2, \xi_2, \phi_2) B_z(\kappa_{21}) g_1(\chi_1, \xi_1, \phi_1) k_1^{s_1} . \qquad (3.9)$$

We note that since $\vec{k}_1^{s_1}$ points along the z axis, and since the external particles are treated as being spinless, we may take $\phi_1 = 0$ with no loss of generality. Furthermore, since z rotations commute

TABLE II. SO(2,1) parametrization of the external momenta.

$$k_{2'}^{F_3} = R_y(\theta_2) B_y(\chi_2) B_x(\xi_2) k_{2'}^{s_2}$$

$$k_{1'}^{F_3} = R_y(\theta_2) B_y(\chi_2) B_x(\xi_2) B_z(\kappa_{21}) R_z(\omega_{12}) B_x(\xi_1) k_{1'}^{s_1}$$

$$k_1^{F_3} = R_y(\theta_2) B_y(\chi_2) B_x(\xi_2) B_z(\kappa_{21}) R_z(\omega_{12}) B_x(\xi_1) k_1^{s_1}$$

$$k_3^{F_3} = B_y(\chi_3) B_x(\xi_3) k_3^{s_3}$$

$$k_5^{F_3} = R_y(\theta_5) B_y(\chi_5) B_x(\xi_5) k_5^{s_5}$$

$$k_4^{F_3} = R_y(\theta_5) B_y(\chi_5) B_x(\xi_5) B_z(\kappa_{54}) R_z(\omega_{45}) B_x(\xi_4) k_4^{s_4}$$

$$k_{4'}^{F_3} = R_y(\theta_5) B_y(\chi_5) B_x(\xi_5) B_z(\kappa_{54}) R_z(\omega_{45}) B_x(\xi_4) k_{4'}^{s_4}$$

$$k_{3'}^{F_3} = B_y(\chi_3) B_x(\xi_3) k_{3'}^{s_3}$$

with z boosts, Eq. (3.9) depends only on the sum $\phi_2 + \chi_1$. We may then set $\phi_2 = 0$ and write $\omega_{12} = \chi_1$. Similarly, we may set $\phi_5 = 0$ and write $\omega_{45} = \chi_4$. The external momenta may then be written in the F_3 frame as shown in Table II.

In order to display the singularity structure of the full amplitude, it is useful to consider the two subamplitudes that result when we treat the lines carrying Q_2 and Q_5 as external particles.[10] These subamplitudes are shown in Fig. 8. In order to help determine the behavior of the group parameters, we introduce the following invariants in addition to those in Eq. (2.1):

$$s_{15} = (Q_1 - Q_3)^2, \quad s_{13} = (k_1 - Q_3)^2,$$
$$s_4 = (k_4 + k_5)^2, \quad s_{25} = (Q_2 + k_5)^2,$$
$$s_{34} = (k_{4'} - Q_3)^2, \quad s_5 = (Q_4 - k_{3'})^2, \qquad (3.10)$$
$$s_{45} = (k_{3'} + k_{4'})^2, \quad s_{14} = (k_{2'} - k_5)^2 .$$

We remark that from Eq. (2.7), the inclusive cross section is a discontinuity in s_X; as a result, the Steinman relation[4,10-12] demands that the inclusive distribution has no discontinuities in s_{15}, s_{13}, s_{25}, s_{34}, etc. It is convenient in specifying the asymptotic limits to define the following use-
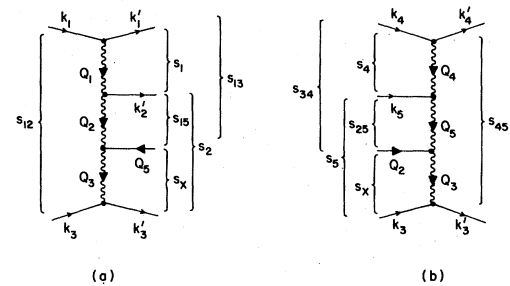

FIG. 8. Invariants defined in text. (a) Invariants to be evaluated with $+i\epsilon$ prescription. (b) Invariants evaluated with $-i\epsilon$ prescription.

TABLE III. SO(2,1) expressions for selected invariant subenergies.

$$s_1 = m_\pi^2 + m_\rho^2 + \frac{\lambda^{1/2}(m_\pi^2, t_1, t_2)\lambda^{1/2}(m_\rho^2, m_\pi^2, t_1)}{-2t_1}\cosh\xi_1 + \frac{(m_\pi^2 + t_1 - t_2)(m_\rho^2 + t_1 - m_\pi^2)}{-2t_1}$$

$$s_{15} = t_1 + t_3 + \frac{(t_5 - t_2 - t_3)(m_\pi^2 - t_1 - t_2)}{-2t_2} - \frac{[-\lambda(t_2, t_3, t_5)]^{1/2}\lambda^{1/2}(m_\pi^2, t_1, t_2)}{-2t_2}\sinh\xi_2$$

$$s_2 = t_1 + m_N^2 + (m_N^2 - \tfrac{1}{4}t_3)^{1/2}\frac{\lambda^{1/2}(m_\pi^2, t_1, t_2)}{\sqrt{-t_2}}\cosh\xi_2\cosh\xi_3\cosh\chi_2 - \frac{\lambda^{1/2}(m_\pi^2, t_1, t_2)[-\lambda(t_2, t_3, t_5)]^{1/2}}{-4t_2}\sinh\xi_2$$

$$- (m_N^2 - \tfrac{1}{4}t_3)^{1/2}\frac{\lambda^{1/2}(m_\pi^2, t_1, t_2)(t_5 - t_2 - t_3)}{(-2t_2)\sqrt{-t_3}}\sinh\xi_2\sinh\xi_3$$

$$- (m_N^2 - \tfrac{1}{4}t_3)^{1/2}\frac{(m_\pi^2 - t_1 - t_2)[-\lambda(t_2, t_3, t_5)]^{1/2}}{(-2t_2)\sqrt{-t_3}}\sinh\xi_3 + \frac{(m_\pi^2 - t_1 - t_2)(t_5 - t_2 - t_3)}{-4t_2}$$

ful quantities:

$$\eta_{12} \equiv s_{12}/s_1 s_2, \quad \eta_{45} \equiv s_{45}/s_4 s_5,$$

$$\eta_{23} \equiv s_2/s_{15}s_X, \quad \eta_{35} \equiv s_5/s_{25}s_X, \tag{3.11}$$

$$\eta_{25} \equiv s_{14}/s_{15}s_{25}.$$

A. Multi-Regge limit

The (unphysical) multi-Regge limit of the expansion shown in Fig. 7 is given by

$$s_1, s_2, s_{12}, s_X, s_{15}, s_{13}, s_4, s_{25}, s_{34}, s_5, s_{45}, s_{14}, \text{ etc.} \to \infty,$$

$$t_1, \ldots, t_5, \eta_{12}, \eta_{45}, \eta_{23}, \eta_{35}, \eta_{25} \text{ finite}. \tag{3.12}$$

In order to determine the behavior of the group parameters in this limit, we can explicitly compute the invariants in Eqs. (2.1) and (3.10) using the expressions in Table II. The results of these explicit calculations for the invariants in Fig. 8(a) are given in Tables III, IV, and V.

We now consider the leading terms in these expressions as $|\xi_1|, |\xi_2|, |\xi_3| \to \infty$. By examining

Tables III, IV, and V, we get

$$s_1 \simeq \frac{\lambda^{1/2}(m_\pi^2, t_1, t_2)\lambda^{1/2}(m_\rho^2, m_\pi^2, t_1)}{-2t_1}\cosh\xi_1, \tag{3.13}$$

$$s_{15} \simeq \frac{[-\lambda(t_2, t_3, t_5)]^{1/2}\lambda^{1/2}(m_\pi^2, t_1, t_2)}{-2t_2}\sinh\xi_2, \tag{3.14}$$

$$s_X \simeq \frac{[-\lambda(t_2, t_3, t_5)]^{1/2}}{\sqrt{-t_3}}(m_N^2 - \tfrac{1}{4}t_3)^{1/2}\sinh\xi_3. \tag{3.15}$$

As a result, we must choose $\xi_2, \xi_3 \to -\infty$. To obtain agreement with standard forms, we choose $\xi_1 \to +\infty$. Our leading terms in the remaining invariants are then

$$s_{13} \simeq \frac{[-\lambda(t_2, t_3, t_5)]^{1/2}\lambda^{1/2}(m_\rho^2, m_\pi^2, t_1)}{16t_1 t_2}$$

$$\times (m_\pi^2 - t_1 - t_2 - 2\sqrt{-t_1}\sqrt{-t_2}\cos\omega_{12})e^{\xi_1 - \xi_2}, \tag{3.16}$$

$$s_2 \simeq \frac{(m_N^2 - \tfrac{1}{4}t_3)^{1/2}\lambda^{1/2}(m_\rho^2, t_1, t_2)}{(-8t_2)\sqrt{-t_3}}$$

$$\times (t_2 + t_3 - t_5 + \sqrt{-t_2}\sqrt{-t_3}\cosh\chi_2)e^{-\xi_2 - \xi_3}, \tag{3.17}$$

TABLE IV. More SO(2,1) expressions for selected invariant subenergies.

$$s_X = m_N^2 + t_2 - \frac{[-\lambda(t_2, t_3, t_5)]^{1/2}}{\sqrt{-t_3}}(m_N^2 - \tfrac{1}{4}t_3)^{1/2}\sinh\xi_3 - \frac{(t_5 - t_2 - t_3)(m_\pi^2 - t_1 - t_2)}{2\sqrt{-t_2}\sqrt{-t_3}}$$

$$s_{13} = m_\pi^2 + t_3 + \frac{(t_5 - t_2 - t_3)\lambda^{1/2}(m_\pi^2, t_1, t_2)}{4t_1 t_2}\lambda^{1/2}(m_\rho^2, m_\pi^2, t_1)\cosh\xi_1$$

$$+ \frac{(t_1 + t_2 - m_\pi^2)[-\lambda(t_2, t_3, t_5)]^{1/2}}{4t_1 t_2}\lambda^{1/2}(m_\rho^2, m_\pi^2, t_1)\cosh\xi_1\sinh\xi_2$$

$$- \frac{[-\lambda(t_2, t_3, t_5)]^{1/2}\lambda^{1/2}(m_\rho^2, m_\pi^2, t_1)}{2\sqrt{-t_1}\sqrt{-t_2}}\sinh\xi_1\cosh\xi_2\cos\omega_{12}$$

$$+ \frac{(t_5 - t_2 - t_3)(m_\pi^2 - t_1 - t_2)(m_\rho^2 - m_\pi^2 - t_1)}{4t_1 t_2}$$

$$+ \frac{(t_1 + m_\pi^2 - m_\rho^2)[-\lambda(t_2, t_3, t_5)]^{1/2}\lambda^{1/2}(m_\pi^2, t_1, t_2)}{4t_1 t_2}\sinh\xi_2$$

$$s_{12} = \frac{(m_N{}^2 - \frac{1}{4}t_3)^{1/2}\lambda^{1/2}(m_\rho{}^2, m_\pi{}^2, t_2)}{32 t_1 t_2 \sqrt{-t_3}}$$

$$\times (t_2 + t_3 - t_5 + 2\sqrt{-t_2}\sqrt{-t_3}\cosh\chi_2)$$

$$\times (m_\pi{}^2 - t_1 - t_2 - 2\sqrt{-t_1}\sqrt{-t_1}\cos\omega_{12})e^{\xi_1 - \xi_2 - \xi_3}.$$

$$(3.18)$$

Then the leading order,

$$\eta_{12} = \frac{m_\pi{}^2 - t_1 - t_2 - 2\sqrt{-t_1}\sqrt{-t_2}\cos\omega_{12}}{\lambda(m_\pi{}^2, t_1, t_2)}$$

$$= \frac{s_{13}}{s_1 s_{15}}, \qquad (3.19)$$

$$\eta_{23} = \frac{t_5 - t_2 - t_3 - 2\sqrt{-t_2}\sqrt{-t_3}\cosh\chi_2}{\lambda(t_2, t_3, t_5)}$$

$$= \frac{s_{12}}{s_{13} s_X}. \qquad (3.20)$$

The last two equations demonstrate the well-known Gram-determinant constraints[10,12] that the subenergies must obey in the multi-Regge limit.

An asymptotic analysis of the invariants shown in Fig. 8(b) would yield further expressions similar to the last five equations.

B. Mueller forward direction (MFD)

We will now calculate the behavior of the group parameters in the case of direct experimental importance, namely the MFD, given by Eq. (2.8). Following Abarbanel and Schwimmer,[6] we note that in the MFD

$$t_1 = t_4, \quad t_2 = t_5. \qquad (3.21)$$

Equations (3.6) imply

$$\cos\theta_2 = \frac{1}{2}\left(\frac{t_3}{t_2}\right)^{1/2}, \quad \sin\theta_2 = \left(1 - \frac{t_3}{4t_2}\right)^{1/2}, \qquad (3.22)$$

$$\theta_2 = -\theta_5. \qquad (3.23)$$

Similarly, Eqs. (3.8) imply that

$$\kappa_{21} = -\kappa_{54}. \qquad (3.24)$$

We can obtain constraints on χ_5 and ξ_5 by setting

TABLE V. SO(2, 1) expression for s_{12}.

$$s_{12} = m_\pi{}^2 + m_N{}^2 + (m_N{}^2 - \tfrac{1}{4}t_3)^{1/2}\frac{\lambda^{1/2}(m_\rho{}^2, m_\pi{}^2, t_1)(m_\pi{}^2 - t_1 - t_2)}{(-2t_1)\sqrt{-t_2}}\cosh\xi_1 \cosh\xi_2 \cosh\xi_3 \cosh\chi_2$$

$$+ (m_N{}^2 - \tfrac{1}{4}t_3)^{1/2}\frac{\lambda^{1/2}(m_\pi{}^2, t_1, t_2)(m_\rho{}^2 - m_\pi{}^2 - t_1)}{(-2t_1)\sqrt{-t_2}}\cosh\xi_2 \cosh\xi_3 \cosh\chi_2$$

$$- \frac{[-\lambda(t_2, t_3, t_5)]^{1/2}\lambda^{1/2}(m_\rho{}^2, m_\pi{}^2, t_1)(m_\pi{}^2 - t_1 - t_2)}{8 t_1 t_2}\cosh\xi_1 \sinh\xi_2$$

$$- \frac{[-\lambda(t_2, t_3, t_5)]^{1/2}(m_\rho{}^2 - m_\pi{}^2 - t_1)\lambda^{1/2}(m_\pi{}^2, t_1, t_2)}{8 t_1 t_2}\sinh\xi_2$$

$$- (m_N{}^2 - \tfrac{1}{4}t_3)^{1/2}\frac{(t_5 - t_2 - t_3)\lambda^{1/2}(m_\rho{}^2, m_\pi{}^2, t_1)(m_\pi{}^2 - t_1 - t_2)}{4 t_1 t_2 \sqrt{-t_3}}\cosh\xi_1 \sinh\xi_2 \sinh\xi_3$$

$$- (m_N{}^2 - \tfrac{1}{4}t_3)^{1/2}\frac{(t_5 - t_2 - t_3)(m_\rho{}^2 - m_\pi{}^2 - t_1)\lambda^{1/2}(m_\pi{}^2, t_1, t_2)}{4 t_1 t_2 \sqrt{-t_3}}\sinh\xi_2 \sinh\xi_3$$

$$- \frac{[-\lambda(t_2, t_3, t_5)]^{1/2}\lambda^{1/2}(m_\rho{}^2, m_\pi{}^2, t_1)}{4\sqrt{-t_1}\sqrt{-t_2}}\sinh\xi_1 \cosh\xi_2 \cos\omega_{12}$$

$$- \frac{(m_N{}^2 - \tfrac{1}{4}t_3)^{1/2}(t_5 - t_2 - t_3)\lambda^{1/2}(m_\rho{}^2, m_\pi{}^2, t_1)}{2\sqrt{-t_1}\sqrt{-t_2}\sqrt{-t_3}}\sinh\xi_1 \cosh\xi_2 \sinh\xi_3 \cos\omega_{12}$$

$$+ \frac{(m_N{}^2 - \tfrac{1}{4}t_3)^{1/2}\lambda^{1/2}(m_\rho{}^2, m_\pi{}^2, t_1)}{\sqrt{-t_1}}\sinh\xi_1 \sinh\xi_2 \cosh\xi_3 \cosh\chi_2 \cos\omega_{12}$$

$$+ \frac{(m_N{}^2 - \tfrac{1}{4}t_3)^{1/2}\lambda^{1/2}(m_\rho{}^2, m_\pi{}^2, t_1)}{\sqrt{-t_1}}\sinh\xi_1 \cosh\xi_3 \sinh\chi_2 \sin\omega_{12}$$

$$- (m_N{}^2 - \tfrac{1}{4}t_3)^{1/2}\frac{[-\lambda(t_2, t_3, t_5)]^{1/2}\lambda^{1/2}(m_\rho{}^2, m_\pi{}^2, t_1)\lambda^{1/2}(m_\pi{}^2, t_1, t_2)}{4 t_1 t_2 \sqrt{-t_3}}\cosh\xi_1 \sinh\xi_3$$

$$+ \frac{(t_5 - t_2 - t_3)\lambda^{1/2}(m_\rho{}^2, m_\pi{}^2, t_1)\lambda^{1/2}(m_\pi{}^2, t_1, t_2)}{8 t_1 t_2}\cosh\xi_1$$

$$- (m_N{}^2 - \tfrac{1}{4}t_3)^{1/2}\frac{[-\lambda(t_2, t_3, t_5)]^{1/2}(m_\rho{}^2 - m_\pi{}^2 - t_1)(m_\pi{}^2 - t_1 - t_2)}{4 t_1 t_2 \sqrt{-t_3}}\sinh\xi_3$$

$$+ \frac{(t_5 - t_2 - t_3)(m_\rho{}^2 - m_\pi{}^2 - t_1)(m_\pi{}^2 - t_1 - t_2)}{8 t_1 t_2}$$

$k_2^{F_3} = k_5^{F_3}$. From Table I, we see that Eqs. (3.21) imply that

$$k_5^{s_5}\big|_{\text{MFD}} = R_y(\pi)k_2^{s_2} . \tag{3.25}$$

Then from Table II and Eq. (3.23), we have

$$R_y(\theta_2)B_y(\chi_2)B_x(\xi_2)k_{2'}^{s_2} = R_y(-\theta_2)B_y(\chi_5)B_x(\xi_5)R_y(\pi)k_{2'}^{s_2} . \tag{3.26}$$

If we explicitly compute the above, equating the t and y components yields

$$\cosh\xi_2\cosh\chi_2 = \cosh\xi_5\cosh\chi_5 ,$$
$$\cosh\xi_2\sinh\chi_2 = \cosh\xi_5\sinh\chi_5 . \tag{3.27}$$

The last two equations yield $\chi_2 = \chi_5$. If we equate the x and z components of Eq. (3.26), we get

$$\sinh\xi_2\cos\theta_2 = \sinh\xi_5\cos\theta_2 , \tag{3.28}$$

$$2(k_{2'}^{s_2})_z\cos\theta_2 = (k_{2'}^{s_2})_t\sin\theta_2(\sinh\xi_2 + \sinh\xi_5) . \tag{3.29}$$

From the condition $k_3 = k_{3'}$ we have $t_3 \to 0$ in the MFD, so that from Eqs. (3.22), we have $\theta_2 = \pi/2$. From Eq. (3.29), we get that $\xi_2 = -\xi_5$. If we demand that Eq. (3.28) holds as t_3 approaches zero, we get that $\xi_2 = \xi_5$, so that we must have $\xi_2 = \xi_5 = 0$. As we shall see in Sec. VI, this last condition has a dramatic interpretation in terms of the cross-channel partial-wave decomposition.

We can fix the remaining group parameters in the MFD by noting that from Tables I and II,

$$k_{1'}^{F_3} = R_y(\pi/2)B_y(\chi_2)B_z(\kappa_{21})R_z(\omega_{12})B_x(\xi_1)k_{1'}^{s_1} ,$$

$$k_{4'}^{F_3} = R_y(-\pi/2)B_y(\chi_2)B_z(-\kappa_{21})R_z(\omega_{45})B_x(\xi_4)R_y(\pi)k_{1'}^{s_1} .$$

The last two equations will be equal if

$$B_z(\kappa_{21})R_z(\omega_{21})B_x(\xi_1) = B_y(-\chi_2)R_y(-\pi)B_y(\chi_2)$$
$$\times B_z(-\kappa_{21})R_z(\omega_{45})B_x(\xi_4)R_y(\pi)$$
$$= B_z(\kappa_{21})R_z(-\omega_{45})B_x(-\xi_4) . \tag{3.30}$$

In the last line, we have used the fact that y boosts commute with y rotations. From Eq. (3.30), we obtain that $\omega_{12} = -\omega_{45}$, $\xi_1 = -\xi_4$. In summary, the MFD is specified by

$$t_1 = t_4, \quad t_2 = t_5, \quad t_3 = 0 ,$$
$$\chi_2 = \chi_5 ,$$
$$\xi_2 = \xi_5 = 0 , \tag{3.31}$$
$$\omega_{12} = -\omega_{45} ,$$
$$\xi_1 = -\xi_4 .$$

The above imply

$$\theta_2 = -\theta_5 = \pi/2 ,$$
$$\kappa_{21} = -\kappa_{54} . \tag{3.32}$$

In the MFD, the external momenta in the F_3 frame are given by

$$k_2^{F_3} = R_y(\pi/2)B_y(\chi_2)k_2^{s_2} ,$$
$$k_{1'}^{F_3} = R_y(\pi/2)B_y(\chi_2)B_z(\kappa_{21})R_z(\omega_{12})B_x(\xi_1)k_{1'}^{s_1} ,$$
$$k_1^{F_3} = R_y(\pi/2)B_y(\chi_2)B_z(\kappa_{21})R_z(\omega_{12})B_x(\xi_1)k_1^{s_1} , \tag{3.33}$$
$$k_2^{F_3} = B_x(\xi_3)k_3^{s_3} ,$$

with similar expressions for the remaining momenta.

If we restrict ourselves to the submanifold of

TABLE VI. SO(2,1) expressions for selected invariants in the MFD.

$$s_1 = m_\pi^2 + m_\rho^2 \frac{\lambda^{1/2}(m_\pi^2, t_1, t_2)\lambda^{1/2}(m_\rho^2, m_\pi^2, t_1)}{-2t_1}\cosh\xi_1 + \frac{(m_\pi^2 + t_1 - t_2)(m_\rho^2 + t_1 - m_\pi^2)}{-2t_1}$$

$$s_{15} = t_1$$

$$s_2 = t_1 + m_N^2 + m_N \frac{\lambda^{1/2}(m_\pi^2, t_1, t_2)}{\sqrt{-t_2}}\cosh\xi_3\cosh\chi_2 - m_N\frac{m_\pi^2 - t_1 - t_2}{\sqrt{-t_2}}\sinh\xi_3$$

$$s_x = m_N^2 + t_2 - 2m_N\sqrt{-t_2}\sinh\xi_3$$

$$s_{13} = m_\pi^2$$

$$s_{12} = m_\pi^2 + m_N^2 + m_N\frac{\lambda^{1/2}(m_\rho^2, m_\pi^2, t_1)(m_\pi^2 - t_1 - t_2)}{(-2t_1)\sqrt{-t_2}}\cosh\xi_1\cosh\xi_3\cosh\chi_2$$
$$+ m_N\frac{\lambda^{1/2}(m_\pi^2, t_1, t_2)(m_\rho^2 - m_\pi^2 - t_1)}{(-2t_1)\sqrt{-t_2}}\cosh\xi_3\cosh\chi_2 + m_N\frac{\lambda^{1/2}(m_\rho^2, m_\pi^2, t_1)}{\sqrt{-t_1}}\sinh\xi\cosh\xi_3\sinh\chi_2\sin\omega_{12}$$
$$+ m_N\frac{\lambda^{1/2}(m_\rho^2, m_\pi^2, t_1)\lambda^{1/2}(m_\pi^2, t_1, t_2)}{2t_1\sqrt{-t_2}}\cosh\xi_1\cosh\xi_3 + \frac{m_N(m_\rho^2 - m_\pi^2 - t_1)(m_\pi^2 - t_1 - t_2)}{2t_1\sqrt{-t_2}}\sinh\xi_3$$

group parameters defined by Eq. (3.31), the forms
of the invariants in Fig. 8(a) become much more
compact. If we use the fact that

$$\frac{[-\lambda(t_2, t_3, t_5)]^{1/2}}{\sqrt{-t_3}} \xrightarrow{\text{MFD}} 2\sqrt{-t_2} \,,$$

then in the MFD the invariants in Tables III, IV,
and V reduce to the expressions in Table VI. If
we take all boost parameters to be large, we have
that

$$s_1 \simeq \frac{\lambda^{1/2}(m_\pi^2, t_1, t_2)\lambda^{1/2}(m_\rho^2, m_\pi^2, t_1)}{-2t_1} \cosh\xi_1 \,,$$

$$s_2 \simeq \frac{\lambda^{1/2}(m_\pi^2, t_1, t_2)}{\sqrt{-t_2}} \cosh\xi_3 \cosh\chi_2 \,, \qquad (3.34)$$

$$s_x \simeq -2m_N\sqrt{-t_2}\sinh\xi_3 \,.$$

In order that the above be large and positive, we
take the limit $\xi_1 \to -\infty$, $\chi_2 \to -\infty$, so that

$$s_{12} \simeq \frac{m_N\lambda^{1/2}(m_\rho^2, m_\pi^2, t_1)}{(-16t_1)\sqrt{-t_2}}$$
$$\times (m_\pi^2 - t_1 - t_2 - 2\sqrt{-t_1}\sqrt{-t_2}\sin\omega_{12})e^{\xi_1-\xi_2-\chi_2} \,.$$

$$(3.35)$$

Then

$$\eta_{12} \simeq \frac{m_\pi^2 - t_1 - t_2 - 2\sqrt{-t_1}\sqrt{-t_2}\sin\omega_{12}}{\lambda(m_\pi^2, t_1, t_2)} \,. \qquad (3.36)$$

It is now clear from the last five equations that
our SO(2, 1) expansion will be an appropriate
asymptotic expansion to describe the reaction of
Fig. 1 in the limit

$$s_{12}, s_1, s_2, s_x, s_2/s_x \to \infty, \quad t_1, t_2, \eta_{12} \text{ fixed.} \quad (3.37)$$

We note that the quantity $s_{13}/s_1 s_{15}$ is independent
of ω_{12}, and $\eta_{12} \neq s_{13}/s_1 s_{15}$, in contrast with Eq.
(3.19). Furthermore, we see that although Eq.
(3.36) depends on $\sin\omega_{12}$, Eq. (3.19) depends on
$\cos\omega_{12}$.

C. Inclusive reaction as a quasiexclusive reaction

In order to see that our equations are reason-
able, it is useful to relate our set of parameters
to those corresponding to a naive set of momenta
as in Fig. 1, treating Q_x as a quasiparticle. Let
the N_2 frame be given by $Q_2^{N_2} = [0, 0, 0, \sqrt{-t_2}]$, and
$p_2^{N_2} = [(p_2^{N_2})_t, 0, 0, (p_2^{N_2})_z]$, where

$$(p_2^{N_2})_z = \frac{t_2 + m_N^2 - s_x}{2\sqrt{-t_2}} \,,$$

$$(p_2^{N_2})_t = \frac{\lambda^{1/2}(t_2, m_N^2, s_x)}{2\sqrt{-t_2}} \,. \qquad (3.38)$$

From Tables I and VI, we have that

$$p_2^{N_2} = B_z(\xi_2)k_3^{s_3} \,, \qquad (3.39)$$

where $k_3^{s_3}$ is evaluated in the limit $t_3 = 0$. For the
rest of our set of "standard" four-momenta, we
choose

$$q^{s_2} = k_2^{s_2}, \quad p_1^{s_1} = k_1^{s_1}, \quad q_1^{s_1} = k_{1'}^{s_1} \,.$$

If we exclusively choose the SO(2, 1) parametriza-
tion of Eq. (3.3a), we may follow steps identical
to the discussion after Eq. (3.9) and write the ex-
ternal momenta in the N_2 frame as

$$p_2^{N_2} = B_z(\xi_3)k_3^{s_3} \,,$$

$$p_1^{N_2} = R_z(\alpha_2)B_x(\beta_2)B_z(\kappa_{21})R_z(\omega_N)B_x(\beta_1)k_1^{s_1} \,,$$

$$q_1^{N_2} = R_z(\alpha_2)B_x(\beta_2)B_z(\kappa_{21})R_z(\omega_N)B_x(\beta_1)k_{1'}^{s_1} \,, \qquad (3.40)$$

$$q^{N_2} = R_z(\alpha_2)B_x(\beta_2)k_{2'}^{s_2} \,.$$

As before, κ_{21} is defined by Eq. (3.8). The angle
ω_N is the Toller angle[9,14] appropriate to the five-
particle amplitude. If we temporarily ignore the
internal degrees of freedom of the missing mass
Q_X, we may set $\alpha_2 = \pi/2$. Now since

$$B_x(\beta_2) = R_z(-\pi/2)B_y(\beta_2)R_z(\pi/2)$$

and

$$B_z(\xi_3) = R_y(-\pi/2)B_y(\xi_3)R_y(\pi/2) \,,$$

then

$$R_y(\pi/2)p_2^{N_2} = B_x(\xi_3)k_3^{s_3} \,,$$

$$R_y(\pi/2)p_1^{N_2} = R_y(\pi/2)B_y(\beta_2)B_z(\kappa_{21})R_z(\omega_N + \pi/2)$$
$$\times B_x(\beta_1)k_1^{s_1} \,,$$

$$R_y(\pi/2)q_1^{N_2} = R_y(\pi/2)B_y(\beta_2)B_z(\kappa_{21})R_z(\omega_N + \pi/2)$$
$$\times B_x(\beta_1)k_{1'}^{s_1} \,, \qquad (3.41)$$

$$R_y(\pi/2)q_2^{N_2} = R_y(\pi/2)B_y(\beta_2)k_{2'}^{s_2} \,.$$

From Eq. (3.33), we can make the identification

$$\beta_2 = \chi_2, \quad \beta_1 = \xi_1, \quad \omega_{12} = \omega_N + \pi/2 \,. \qquad (3.42)$$

We see that in the MFD, the F_2 frame corresponds
to a Breit frame with the momentum Q_2 along the
x axis, rather than along the z axis as in the N_2
frame. Since $\sin\omega_{12} = \cos\omega_N$, Eq. (3.36) depends
on the cosine of the "naive" Toller angle, as
expected. What is surprising is the relation $\beta_2 = \chi_2$,
and in the next three sections we explore the im-
plications of this relation in terms of complex
angular momentum.

IV. THE O(3) EXPANSION AND REGGEIZATION

The asymptotic behavior of M_8 can be deter-
mined by expanding it, using as basis functions
the irreducible unitary representations of the
group SO(2, 1).[15-17] Rather than work with these
less familiar functions, we will find it convenient
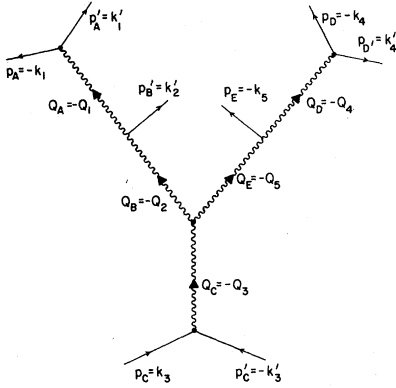and instructive to follow Abarbanel and Schwim-

FIG. 9. Tree diagram symbolizing O(3) parametrization of M_8 obtained by analytic continuation.

mer,[6] and continue our SO(2,1) parametrization of M_8 into a parametrization of O(3). We then can write down an ordinary partial-wave expansion, and directly interpret the asymptotic behavior in terms of complex angular momenta and helicities.

The O(3) expansion symbolized by Fig. 9 is produced by first continuing the amplitude into the kinematic region where $t_1, \ldots, t_5 \geq 0$. If we denote by t_A the value of t_1 reached at the end of the continuation, then since t_A is a physical subenergy above threshold, we must continue to the $+i\epsilon$ boundary of the $+\mathrm{Re}\, t_A$ axis in the complex t_A plane. The net effect of the continuation is summarized by $\sqrt{-t_1} = e^{-i\pi/2}\sqrt{t_A}$, with identical relations for $t_B, \ldots, t_E$.

Let us examine the effect of the continuation on the standard vectors of Table I. After continuation, the four-vector $k_1^{s_1}$ becomes

$$k_1^{s_1} = \left[-i\frac{\lambda^{1/2}(m_\rho^2, m_\pi^2, t_A)}{2\sqrt{t_A}}, 0, 0, -i\frac{t_A + m_\pi^2 - m_\rho^2}{2\sqrt{t_A}} \right]$$
$$= -p_A^{s_1}. \tag{4.1}$$

The quantities appearing in the last equation are still expressed in the Breit frame where $\sqrt{-t_1}$ points along the $+z$ axis. We consider, then, the action of the complex z boost $B_z(-i\pi/2)$, which has the explicit form

$$B_z(-i\pi/2) = \begin{bmatrix} 0 & 0 & 0 & -i \\ 0 & 1 & 0 & 0 \\ 0 & 0 & 1 & 0 \\ -i & 0 & 0 & 0 \end{bmatrix}. \tag{4.2}$$

A new standard frame s_A is defined such that four-vectors in the s_A frame are given by the action of $B_z(-i\pi/2)$ on the four-vectors in the s_1 frame. Then

$$B_z\left(-\frac{i\pi}{2}\right) k_1^{s_1}$$

$$= \left[-\frac{t_A + m_\pi^2 - m_\rho^2}{2\sqrt{t_A}}, 0, 0, -\frac{\lambda^{1/2}(m_\rho^2, m_\pi^2, t_A)}{2\sqrt{t_A}} \right]$$
$$= -p_A^{s_A}. \tag{4.3}$$

If we compare Figs. 7 and 9, we see that the minus sign in the last equation arises from the fact that k_1 is an incoming vector and p_A is an outgoing vector. It is quite apparent that the frame s_A is the center-of-mass frame of p_A and $p_{A'}$, with $p_A^{s_A}$ pointing along the $+z$ axis. If we continue in the remaining $t_B, \ldots, t_E$, such that each is timelike at the end of each continuation, and apply the complex z boost of Eq. (4.2), we generate the set of standard vectors appropriate to Fig. 9. These vectors are given in Table VII.

We can also continue the parameters relating the various Lorentz frames involved in the SO(2,1) expansion. From Eqs. (3.8), we have

$$\cosh\kappa_{21} = \frac{t_B + t_A - m_\pi^2}{2(t_B t_A)^{1/2}}, \quad \sinh\kappa_{21} = -\frac{\lambda^{1/2}(t_B, t_A, m_\pi^2)}{2(t_B t_A)^{1/2}}, \tag{4.4}$$

$$\cosh\kappa_{54} = \frac{t_E + t_D - m_\pi^2}{2(t_E t_D)^{1/2}}, \quad \sinh\kappa_{54} = +\frac{\lambda^{1/2}(t_E, t_D, m_\pi^2)}{2(t_E t_D)^{1/2}}.$$

So we let

$$\kappa_{BA} = -\kappa_{21}, \quad \kappa_{ED} = \kappa_{54}. \tag{4.5}$$

If we choose the path of continuation such that

$$[-\lambda(t_1, t_2, t_3)]^{1/2} = -i\lambda^{1/2}(t_A, t_B, t_C), \tag{4.6}$$

from Eqs. (3.6) we deduce that

$$\cos\theta_2 = \frac{t_C + t_B - t_E}{2\sqrt{t_B}\sqrt{t_E}} \equiv \cosh\theta_B,$$

$$\sin\theta_2 = i\frac{\lambda^{1/2}(t_B, t_C, t_E)}{2\sqrt{t_B}\sqrt{t_E}} \equiv i\sinh\theta_B,$$

$$\cos\theta_5 = \frac{t_C + t_E - t_B}{2\sqrt{t_C}\sqrt{t_E}} \equiv \cosh\theta_E, \tag{4.7}$$

$$\sin\theta_5 = -i\frac{\lambda^{1/2}(t_B, t_C, t_E)}{2\sqrt{t_C}\sqrt{t_E}} \equiv -i\sinh\theta_E.$$

We then define $\theta_2 \equiv i\theta_B$ and $\theta_5 \equiv -i\theta_E$.

Now according to the Bargmann-Hall-Wightmann theorem,[15] M_8 should be invariant under the complex Lorentz transformation $B_z(-i\pi/2)$. If we explicitly display the dependence of M_8 on the external momenta in the F_3 frame, we have the relation

$$M_i(k_1^{F_3}, k_1^{F_3}, \ldots, k_5^{F_3})$$

$$= M_8\left(B_z\left(-\frac{i\pi}{2}\right)k_1^{F_3}, B_z\left(-\frac{i\pi}{2}\right)k_1^{F_3}, \ldots, B_z\left(-\frac{i\pi}{2}\right)k_5^{F_3} \right).$$
$$\tag{4.8}$$

TABLE VII. Reference momenta for the O(3) parametrization $[x = (t, \vec{x})]$.

$$B_z\left(-\frac{i\pi}{2}\right)k_1^{s1} = \left[-\frac{t_A + m_\pi^2 - m_\rho^2}{2\sqrt{t_A}}, 0, 0, -\frac{\lambda^{1/2}(m_\rho^2, m_\pi^2, t_A)}{2\sqrt{t_A}}\right] = -p_A^{sA}$$

$$B_z\left(-\frac{i\pi}{2}\right)k_{1'}^{s1} = \left[\frac{t_A + m_\rho^2 - m_\pi^2}{2\sqrt{t_A}}, 0, 0, -\frac{\lambda^{1/2}(m_\rho^2, m_\pi^2, t_A)}{2\sqrt{t_A}}\right] = p_{A'}^{sA}$$

$$B_z\left(-\frac{i\pi}{2}\right)k_2^{s2} = \left[-\frac{t_B + t_A - m_\pi^2}{2\sqrt{t_B}}, 0, 0, \frac{\lambda^{1/2}(m_\pi^2, t_A, t_B)}{2\sqrt{t_B}}\right] = -p_B^{sB}$$

$$B_z\left(-\frac{i\pi}{2}\right)k_{2'}^{s2} = \left[\frac{t_B + m_\pi^2 - t_A}{2\sqrt{t_B}}, 0, 0, \frac{\lambda^{1/2}(m_\pi^2, t_A, t_B)}{2\sqrt{t_B}}\right] = p_{B'}^{sB}$$

$$B_z\left(-\frac{i\pi}{2}\right)k_3^{s3} = [\tfrac{1}{2}\sqrt{t_C}, 0, 0, -(t_C/4 - m_N^2)^{1/2}] = p_C^{sC}$$

$$B_z\left(-\frac{i\pi}{2}\right)k_{3'}^{s3} = [-\tfrac{1}{2}\sqrt{t_C}, 0, 0, -(t_C/4 - m_N^2)^{1/2}] = -p_{C'}^{sC}$$

$$B_z\left(-\frac{i\pi}{2}\right)k_4^{s4} = \left[-\frac{t_D + m_\rho^2 - m_\pi^2}{2\sqrt{t_D}}, 0, 0, -\frac{\lambda^{1/2}(m_\pi^2, m_\rho^2, t_D)}{2\sqrt{t_D}}\right] = -p_D^{sD}$$

$$B_z\left(-\frac{i\pi}{2}\right)k_{4'}^{s4} = \left[\frac{t_D + m_\pi^2 - m_\rho^2}{2\sqrt{t_D}}, 0, 0, \frac{\lambda^{1/2}(m_\pi^2, m_\rho^2, t_D)}{2\sqrt{t_D}}\right] = p_{D'}^{sD}$$

$$B_z\left(-\frac{i\pi}{2}\right)k_5^{s5} = \left[-\frac{t_E + m_\pi^2 - t_D}{2\sqrt{t_E}}, 0, 0, -\frac{\lambda^{1/2}(m_\pi^2, t_D, t_E)}{2\sqrt{t_E}}\right] = -p_E^{sE}$$

$$B_z\left(-\frac{i\pi}{2}\right)k_{5'}^{s5} = \left[\frac{t_E + t_D - m_\pi^2}{2\sqrt{t_E}}, 0, 0, \frac{\lambda^{1/2}(m_\pi^2, t_D, t_E)}{2\sqrt{t_E}}\right] = p_{E'}^{sE}$$

Note that the momenta on the left-hand side of Eq. (4.8) are evaluated in the Breit frame where $\sqrt{-t_3}$ lies along the z axis, while on the right-hand side the momenta are evaluated in the frame where $\sqrt{t_C}$ is the center-of-mass energy.

In order to completely define the continuation of our SO(2, 1) parameters into our O(3) parameters, we will utilize the following relations, which may be verified by explicit matrix multiplication:

$$B_z(-i\pi/2)B_y(\chi)B_z(i\pi/2) = R_x(-i\chi),$$

$$B_z(-i\pi/2)B_x(\xi)B_z(i\pi/2) = R_y(i\xi), \qquad (4.9)$$

$$B_z(-i\pi/2)R_y(\theta)B_z(i\pi/2) = B_x(i\theta).$$

We illustrate the general procedure by evaluating $B_z(-i\pi/2)k_1^{F3}$. We will attempt to reduce all the boosts containing our SO(2, 1) parameters into complex rotations. Then

$$B_z\left(-\frac{i\pi}{2}\right)k_1^{F3} = B_z\left(-\frac{i\pi}{2}\right)R_y(\theta_2)B_y(\chi_2)B_x(\xi_2)B_z(\kappa_{21})$$

$$\times R_z(\omega_{12})B_x(\xi_1)B_z\left(\frac{i\pi}{2}\right)p_A^{s_k}$$

$$= B_z(-\theta_B)R_z(-i\chi_2)R_x(-i\chi_2)R_y(i\xi_2)$$

$$\times B_z(\omega_{12})R_y(i\xi_1)p_A^{sA}. \qquad (4.10)$$

Since z boosts commute with z rotations, $R_z(\omega_{12})$ commutes with the Lorentz transformation that takes us from the t_3 Breit frame to the t_C center-of-mass frame. The well-known fact[14] that ω_{12},

the Toller angle, is a physical angle after continuation is elegantly demonstrated.

As in Ref. 6, we now must specify the momenta entirely in terms of y and z rotations, in order to express M_8 in terms of the standard basis functions for the rotation group. Then since

$$R_y\left(\frac{\pi}{2}\right)R_x(\chi)R_y\left(-\frac{\pi}{2}\right) = R_z(-\chi), \qquad (4.11)$$

Eq. (4.10) becomes

$$R_y\left(\frac{\pi}{2}\right)B_z\left(-\frac{i\pi}{2}\right)k_{1'}^{F3} = B_z(\theta_B)R_z(i\chi_2)R_y\left(i\xi_2 + \frac{\pi}{2}\right)$$

$$\times B_z(-\kappa_{AB})R_z(\omega_{12})R_y(i\xi_1)p_A^{sA}.$$

Similar calculations on the other momenta listed in Table II dictate the following choice of O(3) parameters:

$$\chi_B = i\chi_2, \quad \chi_C = i\chi_3, \quad \chi_E = i\chi_5,$$

$$\xi_A = i\xi_1, \quad \xi_B = i\xi_2, \quad \xi_C = i\xi_3, \quad \xi_D = i\xi_4, \qquad (4.12)$$

$$\xi_E = i\xi_5, \quad \omega_{AB} = \omega_{12}, \quad \omega_{DE} = \omega_{45}.$$

We can now complete our specification of the O(3) parametrization of M_8 by giving expressions for the external momenta in the F_C frame. The F_C frame will be defined by specifying the components of any four-vector V in F_C in terms of its components in the F_3 frame:

$$V^{F_C} = R_y\left(\frac{\pi}{2}\right) B_z \left(-\frac{i\pi}{2}\right) V^{F_3}. \qquad (4.13)$$

The parametrization of our external momenta in the F_C frame is therefore fixed and given in Table VIII.

Further insight into the nature of the O(3) variables is gained by specifying the additional

frames F_A, F_B, F_D, F_E, in which the respective conditions $\vec{Q}_A^{F_A} = \vec{Q}_B^{F_B} = \vec{Q}_D^{F_D} = \vec{Q}_E^{F_E} = 0$ hold. We can choose the orientations of the coordinate axes in these frames so that the ξ's correspond to polar angles, and the χ's and ω's correspond to azimuthal angles. The F_C frame, determined by Eq. (4.13), is shown in Fig. 10. We give the coordinates of the following vectors in that frame:

$$Q_B^{F_C} = [\sqrt{t_B}\cosh\theta_B, 0, 0, \sqrt{t_B}\sinh\theta_B],$$

$$p_C^{F_C} = \left[(p_C^{F_C})_t, -|\vec{p}_C^{F_C}|\sin\left(\xi_C+\frac{\pi}{2}\right)\cos\chi_C, -|\vec{p}_C^{F_C}|\sin\left(\xi_C+\frac{\pi}{2}\right)\sin\chi_C, -|\vec{p}_C^{F_C}|\cos\left(\xi_C+\frac{\pi}{2}\right)\right]. \qquad (4.14)$$

The vector $\vec{Q}_B^{F_C}$ defined the z axis, so that $\xi_C+\pi/2$ is the polar angle of $\vec{p}_C^{F_C}$ and χ_C is its azimuthal angle. For convenience, we may set $\chi_C=0$, so that $\vec{p}_C^{F_C}$ lies in the half-plane $y=0$, $x \leqslant 0$.

Next, we define the F_B frame, shown in Fig. 11. The orientation of the coordinate axes is specified by the vectors

$$Q_C^{F_B} = [\sqrt{t_C}\cosh\theta_B, 0, 0, -\sqrt{t_C}\sinh\theta_B],$$

$$p_{B'}^{F_B} = \left[(p_{B'}^{F_B})_t, |\vec{p}_{B'}^{F_B}|\sin\left(\xi_B+\frac{\pi}{2}\right)\cos\chi_B, |\vec{p}_{B'}^{F_B}|\sin\left(\xi_B+\frac{\pi}{2}\right)\sin\chi_B, |\vec{p}_{B'}^{F_B}|\cos\left(\xi_B+\frac{\pi}{2}\right)\right]. \qquad (4.15)$$

So $\vec{Q}_C^{F_B}$ defines the $-z$ axis, and $\xi_B+\pi/2$ is the polar angle of $p_{B'}^{F_B}$, and χ_B is the azimuthal angle. Since we have set $i\chi_3=\chi_C=0$ in Sec. III, $\vec{p}_C^{F_B}$ and $\vec{p}_{C'}^{F_B}$ will lie in the x-z plane. In Sec. V, we will make use of the fact that in the MFD, given by Eq. (3.31), we will set $\xi_B=-i\xi_2=0$, so that χ_B becomes the angle between $\vec{p}_{B'}^{F_B}$ and the $+x$ axis.

Finally, in Fig. 12, we show the F_A frame. We have

$$p_{B'}^{F_A} = [(p_{B'}^{F_A})_t, 0, 0, (p_{B'}^{F_A})_z],$$

$$p_A^{F_A} = [(p_A^{F_A})_t, |\vec{p}_A^{F_A}|\sin\xi_A\cos\omega_{AB}, |\vec{p}_A^{F_A}|\sin\xi_A\sin\omega_{AB}, |\vec{p}_A^{F_A}|\cos\xi_A]. \qquad (4.16)$$

The z axis is defined by $\vec{p}_{B'}^{F_A}$, ξ_A is the polar angle of $\vec{p}_A^{F_A}$, and ω_{AB} is its azimuthal angle. Similar configurations are found in the F_D and F_E frames, with ξ_D and $\xi_E+\pi/2$ corresponding to polar angles, and ω_{DE} and χ_E corresponding to azimuthal angles.

Having specified the nature of the angles corresponding to our set of O(3) parameters, we now examine their behavior in the various asymptotic limits of Sec. II. Let us define the (unphysical) multi-Regge limit in terms of the invariants by

$$s_1, s_{15}, s_X, s_4, s_{25} \to \infty,$$

$$s_{13}, s_2, s_{34}, s_5, \text{etc.} \to \infty,$$

$$s_{12}, s_{45}, \text{etc.} \to \infty,$$

$$t_1, t_2, t_3, t_4, t_5, \eta_{12}, \xi_{45}, \eta_{23}, \eta_{35}, \eta_{25} \text{ fixed.}$$

The first line consists of those invariants that span one wavy line in Fig. 9 (see Fig. 8). The second line consists of those that span two wavy lines, and the third, three or more. From Eqs. (3.13) to (3.20), and their counterparts for the other invariants, we have that $|\xi_1|, |\xi_2|, \ldots, |\xi_5|$ become large, while $\chi_2, \chi_5, \omega_{12}$, and ω_{45} remain finite. In terms of the O(3) parameters, we must have that the polar angles $|\xi_A|, |\xi_B|, |\xi_C|, |\xi_D|$, and $|\xi_E|$ become large, while the azimuthal angles $\chi_B, \chi_E, \omega_{AB}$, and ω_{DE} remain finite.[6,10] Let us recall the reasons for terming this the multi-Regge limit.

For the moment, we let χ_c be nonzero and write the O(3) expansion of M_8, as in Ref. 10. If we are cavalier about minus signs and phases, we have

$$M_8 = \sum_{\lambda_A=-\infty}^{+\infty} \sum_{J_A, J_B=|\lambda_A|}^{\infty} \sum_{\lambda_B=-J_B}^{+J_B} \sum_{\lambda_D=-\infty}^{+\infty} \sum_{J_D, J_E=|\lambda_D|}^{\infty} \sum_{\lambda_E=-J_E}^{+J_E} \sum_{J_C=|\lambda_B+\lambda_E|}^{\infty} e^{i\lambda_A\omega_{AB}}e^{i\lambda_B\chi_B}e^{i\lambda_D\omega_{DE}}e^{i\lambda_E\chi_E}e^{i\lambda_C\chi_C}$$

$$\times d_{0\lambda_A}^{J_A}(\xi_A)d_{\lambda_A\lambda_B}^{J_B}\left(\xi_B+\frac{\pi}{2}\right)d_{0\lambda_D}^{J_D}(\xi_D)d_{\lambda_D,\lambda_E}^{J_E}\left(\xi_E+\frac{\pi}{2}\right)d_{\chi_C0}^{J_C}\left(\xi_C+\frac{\pi}{2}\right)A_{\lambda_A\lambda_B\lambda_C\lambda_D\lambda_E}^{J_A J_B J_C J_D J_E}(t_A, \ldots, t_E). \qquad (4.17)$$

TABLE VIII. O(3) parametrization of the momenta.

$$p_B^{F_C} = B_z(\theta_B)R_z(\chi_B)R_y(\xi_B + \pi/2)p_B^{S_B},$$

$$p_{A'}^{F_C} = B_z(\theta_B)R_z(\chi_B)R_y(\xi_B + \pi/2)B_z(-\kappa_{BA})R_z(\omega_{AD})R_y(\xi_A)p_{A'}^{S_A}$$

$$p_A^{F_C} = B_z(\theta_B)R_z(\chi_B)R_y(\xi_B + \pi/2)B_z(-\kappa_{BA})R_z(\omega_{AD})R_y(\xi_A)p_A^{S_A}$$

$$p_C^{F_C} = R_z(\chi_C)R_y(\xi_C + \pi/2)p_C^{S_C}$$

$$p_E^{F_C} = B_z(-\theta_E)R_z(\chi_E)R_y(\xi_E + \pi/2)p_E^{S_E}$$

$$p_D^{F_C} = B_z(-\theta_E)R_z(\chi_E)R_y(\xi_E + \pi/2)B_z(\kappa_{ED})R_z(\omega_{DE})R_y(\xi_D)p_D^{S_D}$$

$$p_{D'}^{F_C} = B_z(-\theta_E)R_z(\chi_E)R_y(\xi_E + \pi/2)B_z(\kappa_{ED})R_z(\omega_{DE})R_y(\xi_D)p_{D'}^{S_D}$$

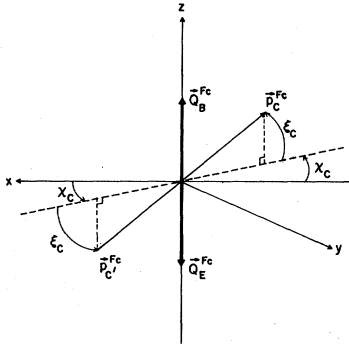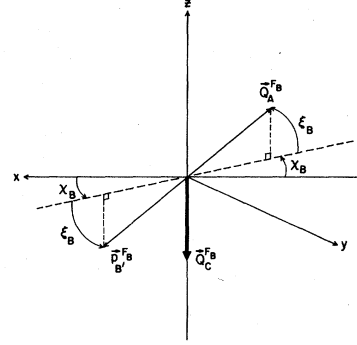$$p_{C'}^{F_C} = R_z(\chi_C)R_y(\xi_C + \pi/2)p_{C'}^{S_C}$$

By rotational invariance,

$$A_{\lambda_A \ldots \lambda_E}^{J_A \ldots J_E}(t_A, \ldots, t_E)$$

vanishes unless $\lambda_B + \lambda_E + \lambda_C = 0$. As was pointed out in Ref. 10, and as we can see from Eqs. (3.16) to (3.20), to leading order the invariants depend on $\cos\omega_{12}$, $\cosh\chi_2$, $\cos\omega_{45}$, and $\cosh\chi_5$. In terms of the O(3) variables, the invariants will depend to leading order on $\cos\omega_{AB}$, $\cos\chi_B$, $\cos\omega_{DE}$, and $\cos\chi_E$. One can then take linear combinations of the partial-wave amplitudes that are even under $\lambda_A \to -\lambda_A$, $\lambda_B \to -\lambda_B$, $\lambda_D \to -\lambda_D$, and $\lambda_E \to -\lambda_E$ (since we are only concerned about the part of M_8 that has a discontinuity in s_X, we need not worry about λ_C). Motivated by Eq. (3.19), we perform the heuristic replacements

$$\cos\lambda_A \omega_{AB} \to (\cos\omega_{AB})^{\lambda_A} \to (-\eta_{12})^{\lambda_A}. \qquad (4.18)$$

Clearly, each step involves a resummation of the series, and a redefinition of the partial-wave amplitude. In the same spirit, we make the additional replacements

FIG. 11. Orientation of vectors in the F_B frame.

$$\cos\lambda_B\chi_B \sim (-\eta_{23})^{\lambda_B}, \quad \cos\lambda_D\omega_{DE} \sim (-\eta_{45})^{\lambda_D},$$

$$\cos\lambda_E\chi_E \sim (-\eta_{35})^{\lambda_E},$$

$$d_{0\lambda_A}^{J_A}(\xi_A) \sim (-s_1)^{J_A}, \quad d_{\lambda_A\lambda_B}^{J_B}\left(\xi_B + \frac{\pi}{2}\right) \sim (-s_{15})^{J_B}, \qquad (4.19)$$

$$d_{\lambda_C 0}^{J_C}\left(\xi_C + \frac{\pi}{2}\right) \sim (-s_X)^{J_C}, \quad d_{00D}^{J_D}(\xi_D) \sim (-s_4)^{J_D},$$

$$d_{\lambda_D\lambda_E}^{J_E}\left(\xi_E + \frac{\pi}{2}\right) \sim (-s_{25})^{J_E}.$$

We now can describe in general terms the procedure for Reggerizing the sum in (4.17). As in standard treatments,[5,6,10,19] "kinematic" singularities in helicity may be removed from the d functions after breaking up the helicity sums in the appropriate fashion.[10,19] The various sums contributing to (4.17) may be rewritten as integrals over complex helicities and angular momenta. In the multi-Regge limit, the invariants associated with the d functions in (4.19) become large, so that the asymptotic behavior of M_8 is obtained by sweeping back the angular momentum contours, and picking up the residues at the leading poles. In Sec. V, we will describe the Reggeization procedure in more detail, and discuss the

FIG. 10. Orientation of vectors in the F_C frame.
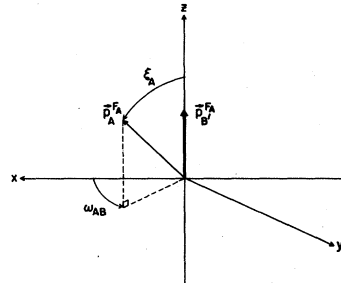
FIG. 12. Orientation of vectors in the F_A frame.

problem of relating the multi-Regge and HPRP limits of M_8.

V. REGGEIZATION AND FACTORIZATION

Before discussing the Reggeization procedure for M_8, we will discuss the equivalent procedure for the linear six-particle amplitude of Fig. 8(a), treating Q_D as a spinless external particle. We will denote this amplitude by M_6. Now in addition to the invariant quantities in (3.11), we define the following:

$$\eta'_{12} \equiv \frac{s_{13}}{s_1 s_{15}}, \quad \eta'_{23} \equiv \frac{s_{12}}{s_{13} s_X},$$

$$\Phi_2 \equiv \frac{s_{12} s_{15}}{s_1 s_{13}} = \frac{\eta_{12}}{\eta'_{12}} = \frac{\eta'_{23}}{\eta_{23}}. \tag{5.1}$$

Owing to Gram-determinant constraints,[13] in the multi-Regge limit we have

$$\eta'_{12} = \eta_{12}, \quad \eta'_{23} = \eta_{23}, \tag{5.2}$$

$$\Phi_2 = 1.$$

The above have already been verified by explicit calculation in (3.19) and (3.20).

The partial-wave expansion of M_6 is given in terms of our O(3) variables for M_8 by

$$M_6 = \sum_{\lambda_A=-\infty}^{+\infty} \sum_{\lambda_B=-\infty}^{+\infty} \sum_{J_A=|\lambda_A|}^{\infty} \sum_{J_C=|\lambda_B|}^{\infty} \sum_{J_B=\max(|\lambda_A|,|\lambda_B|)}^{\infty} e^{i\lambda_A \omega_{AB}} e^{i\lambda_B \chi_B} d_{0\lambda_A}^{J_B}(\xi_A) d_{\lambda_A\lambda_B}^{J_B}\left(\xi_B+\frac{\pi}{2}\right) d_{\lambda_B 0}^{J_C}\left(\xi_C+\frac{\pi}{2}\right)$$

$$\times A_{\lambda_A\lambda_B}^{J_A J_B J_C}(t_A, t_B, t_C). \tag{5.3}$$

In order to perform the necessary Sommerfeld-Watson transformation on the partial-wave sum, we divide the sum up so that the partial-wave amplitudes are free of "kinematic" singularities in the helicities λ_A and λ_B.[6,10,19] If, in (4.18) and (4.19), we may write

$$M_6 = M_{6<} + M_{6>}$$

$$= \sum_{\lambda_A>\lambda_B\geq 0} \sum_{J_A=\lambda_A}^{\infty} \sum_{J_C=\lambda_B}^{\infty} \sum_{J_B=\lambda_A}^{\infty} Z_{12}^{\lambda_A} Z_{23}^{\lambda_B} d_{0\lambda_A}^{J_A}(\xi_A) d_{\lambda_A\lambda_B}^{J_B}\left(\xi_B+\frac{\pi}{2}\right) d_{\lambda_B 0}^{J_C}\left(\xi_C+\frac{\pi}{2}\right) A_{\lambda_A\lambda_B}^{J_A J_B J_C}(t_A, t_B, t_C)_<$$

$$+ \sum_{\lambda_B\geq\lambda_A\geq 0} \sum_{J_A=\lambda_A}^{\infty} \sum_{J_C=\lambda_B}^{\infty} \sum_{J_B=\lambda_B}^{\infty} Z_{12}^{\lambda_A} Z_{23}^{\lambda_B} d_{0\lambda_A}^{J_A}(\xi_A) d_{\lambda_A\lambda_B}^{J_B}\left(\xi_B+\frac{\pi}{2}\right) d_{\lambda_B 0}^{J_C}\left(\xi_C+\frac{\pi}{2}\right) A_{\lambda_A\lambda_B}^{J_A J_B J_C}(t_A, t_B, t_C)_>, \tag{5.4}$$

where

$$Z_{12} = \eta_{12} \text{ or } \eta'_{12} \text{ and } Z_{23} = \eta_{23} \text{ or } \eta'_{23}. \tag{5.5}$$

The subscript < denotes continuation away from $\lambda_B < \lambda_A$, and the subscript > denotes the continuation away from $\lambda_B \geq \lambda_A$. The possibility ambiguity in the choice of the η's in the multi-Regge limit is due to the relations in (5.2). If we extract the kinematic singularities from the d functions and perform the substitutions of (4.19), we may write the following integral representations [see Eq. (4.5) of Ref. 5]:

$$M_{6<}^{\tau_A \tau_B \tau_C} = \frac{1}{(2\pi i)^5} \int d\lambda_B \int d\lambda_A \int dJ_A dJ_B dJ_C \Gamma(\lambda_A - J_A)\Gamma(-\lambda_A) \frac{\Gamma(\lambda_A - J_B)\Gamma(\lambda_B - J_B)}{\Gamma(-J_B)} \Gamma(-\lambda_B)\Gamma(\lambda_B - J_C)$$

$$\times \frac{\sin\pi(\lambda_B - J_B)\sin\pi\lambda_A}{\sin\pi J_B \sin\pi(\lambda_B - \lambda_A)}(-Z_{12})^{\lambda_A}(-Z_{23})^{\lambda_B}$$

$$\times (-s_1)^{J_A}(-s_{15})^{J_B}(-s_X)^{J_C} A_{\lambda_A\lambda_B}^{J_A J_B J_C}(t_A, t_B, t_C)_<, \tag{5.6}$$

$$M_{6>}^{\tau_A \tau_B \tau_C} = \frac{1}{(2\pi i)^5} \int d\lambda_A \int d\lambda_B \int dJ_A dJ_B dJ_C \Gamma(\lambda_A - J_A)\Gamma(-\lambda_A) \frac{\Gamma(\lambda_B - J_B)\Gamma(\lambda_B - J_B)}{\Gamma(-J_B)} \Gamma(-\lambda_B)\Gamma(\lambda_B - J_C)$$

$$\times \frac{\sin\pi(\lambda_A - J_B)\sin\pi\lambda_B}{\sin\pi J_B \sin\pi(\lambda_A - \lambda_B)}(-Z_{12})^{\lambda_A}(-Z_{23})^{\lambda_B}$$

$$\times (-s)^{J_A}(-s_{15})^{J_B}(-s_X)^{J_C} A_{\lambda_A\lambda_B}^{J_A J_B J_C}(t_A, t_B, t_C)_>. \tag{5.7}$$

We will carefully specify the locations of the helicity contours shortly, but we note that all contours are determined by the requirement that when they are pushed to the right, the partial-wave sums must be reproduced.[5,20] As a result, the dynamical poles in J_A, J_B, and J_C must lie to the left of the angular momentum contours. Now if we write the pole contributions to the partial-wave amplitudes as

$$A_{\lambda_A \lambda_B}^{J_A J_B J_C}(t_A, t_B, t_C)_< = \frac{b_<(\lambda_A, \lambda_B; \Phi_2)}{(J_A - \alpha_A)(J_B - \alpha_B)(J_C - \alpha_C)},$$

$$A_{\lambda_A \lambda_B}^{J_A J_B J_C}(t_A, t_B, t_C)_> = \frac{b_>(\lambda_A, \lambda_B; \Phi_2)}{(J_A - \alpha_A)(J_B - \alpha_B)(J_C - \alpha_C)},$$

(5.8)

the residues $b_<$ and $b_>$ depend on λ_A, λ_B, t_A, t_B, t_C, and (possibly) Φ_2. We can sweep the J_A, J_B, and J_C contours to the left in (5.6) and (5.7), and obtain

$$M_{6<}^{\tau_A \tau_B \tau_C} = \frac{(-s_1)^{\alpha_A}(-s_{15})^{\alpha_B}(-s_X)^{\alpha_C}}{(2\pi i)^2} \int_{C_{\lambda_B}^<} d\lambda_B \int_{C_{\lambda_A}^<} d\lambda_A \Gamma(\lambda_A - \alpha_A)\Gamma(\lambda_A - \alpha_B)\Gamma(-\lambda_B)\Gamma(\lambda_B - \alpha_C)$$

$$\times \frac{\pi}{\sin\pi(\lambda_B - \lambda_A)} (-Z_{12})^{\lambda_A}(-Z_{23})^{\lambda_B}$$

$$\times \frac{\Gamma(\alpha_B + 1)}{\Gamma(\alpha_B - \lambda_B + 1)} \frac{b_<(\lambda_A, \lambda_B; \Phi_2)}{\Gamma(\lambda_A + 1)},$$

(5.9)

$$M_{6>}^{\tau_A \tau_B \tau_C} = \frac{(-s_1)^{\alpha_A}(-s_{15})^{\alpha_B}(-s_X)^{\alpha_C}}{(2\pi i)^2} \int_{C_{\lambda_A}^>} d\lambda_A \int_{C_{\lambda_B}^>} d\lambda_B \Gamma(\lambda_A - \alpha_A)\Gamma(-\lambda_A)\Gamma(\lambda_B - \alpha_B)\Gamma(\lambda_B - \alpha_C)$$

$$\times \frac{\pi}{\sin\pi(\lambda_A - \lambda_B)} (-Z_{12})^{\lambda_A}(-Z_{23})^{\lambda_B}$$

$$\times \frac{\Gamma(\alpha_B + 1)}{\Gamma(\alpha_B - \lambda_A + 1)} \frac{b_>(\lambda_A, \lambda_B; \Phi_2)}{\Gamma(\lambda_B + 1)}.$$
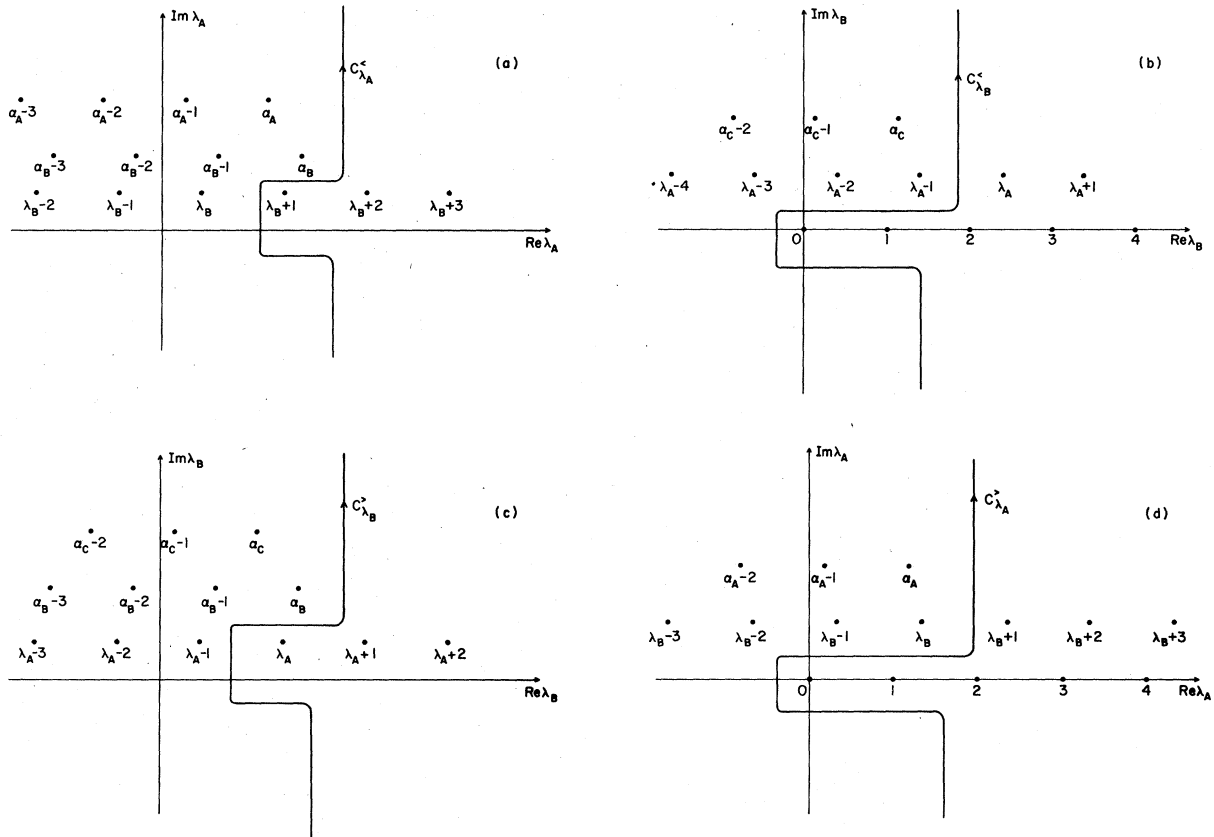
(5.10)

FIG. 13. Helicity contours used to define $M_{6<}^{\tau_A \tau_B \tau_C}$ and $M_{6>}^{\tau_A \tau_B \tau_C}$. (a) Contour $C_{\lambda_A}^<$ which reproduces the sum for $\lambda_B < \lambda_A$. (b) Contour $C_{\lambda_B}^<$ which reproduces the sum for $\lambda_B < \lambda_A$. (c) Contour $C_{\lambda_B}^>$ which reproduces the sum for $\lambda_B \geq \lambda_A$. (d) Contour $C_{\lambda_A}^>$ which reproduces the sum for $\lambda_B \geq \lambda_A$.

In the above, we have made liberal use of the identity

$$\Gamma(x)\Gamma(1-x)=\pi/\sin\pi x. \tag{5.11}$$

The four helicity contours $C_{\lambda_B}^<$, $C_{\lambda_A}^<$, $C_{\lambda_B}^<$, $C_{\lambda_A}^<$ are shown in Figs. 13(a)–13(d).

From (5.9) and (5.10), we see that the multi-Regge limit is a "pure" Regge limit in the sense that the leading power behavior in the large invariants s_1, s_{15}, and s_X, is determined by the poles in angular momenta; this, of course, can be traced to the fact that from (3.13), (3.14), (3.15), and (4.12), these invariants are proportional to the cosines of polar angles.

Let us now investigate the cut structure of (5.9) and (5.10). From Fig. 8, we see that s_1 and s_{15} overlap; so do s_{15} and s_X. Since the Steinmann relation[11,12] forbids simultaneous discontinuities in overlapping channel invariants, the integrals in (5.9) and (5.10) must contain singularities that exactly cancel the overlapping cuts. If we sweep the helicity contours to the left in Figs. 13(a)–13(d), it turns out that the locations of the poles in the complex helicity planes are fixed by the "kinematic" Γ functions in such a way that the Steinmann relations are satisfied. As pointed out in Ref. 5, due to considerable resummation of series, etc., the derivations of representations such as (5.9) and (5.10) are not entirely convincing. Indeed, the fact that the extraction procedure leads to a representation that satisfies the Steinmann relation is one of the main justifications of the procedure.

To illustrate the points raised in the last paragraph, let us invoke the Steinmann relation to show that in $M_{6<}^{T_A T_B T_C}$, we must choose $Z_{12}=\eta_{12}'$ and

$Z_{23}=\eta_{23}'$. To see this, consider the contributions from the leading helicity poles at $\lambda_A=\alpha_A$ and $\lambda_B=\alpha_C$ that arise when we sweep $C_{\lambda_A}^<$ and $C_{\lambda_B}^<$ to the left in Fig. 13(a) and 13(b). These poles give rise to a term

$$M_{6<}^{T_A T_B T_C} \sim (-s_1)^{\alpha_A}(-s_{15})^{\alpha_B}(-s_X)^{\alpha_C}\Gamma(-\alpha_C)\Gamma(\alpha_C-\alpha_B)$$
$$\times\Gamma(\alpha_B-\alpha_A)(-Z_{12})^{\alpha_B}(-Z_{23})^{\alpha_C}b_>(\alpha_B,\alpha_C;\Phi_2). \tag{5.12}$$

The choice $Z_{12}=\eta_{12}$ and $Z_{23}=\eta_{23}$ leads to simultaneous discontinuities in s_1 and s_{15} and in s_1 and s_2. On the other hand, the choice $Z_{12}=\eta_{12}'$ and $Z_{23}=\eta_{23}'$ gives a leading behavior in the invariants of the form

$$(-s_1)^{\alpha_A-\alpha_B}(-s_{13})^{\alpha_B-\alpha_C}(-s_{12})^{\alpha_C}.$$

The above gives rise to an admissible cut structure since from Fig. 8(a) we have that s_1, s_{13}, and s_{12} do not overlap. The locations of the helicity poles in (5.9) are such that they produce terms that exactly cancel the overlapping cuts. Similarly, if we examine the contributions to (5.10) from the helicity poles at $\lambda_A=\alpha_A$ and $\lambda_B=\alpha_B$, we see that we must set $Z_{12}=\eta_{12}$ and $Z_{23}=\eta_{23}$.

Pursuing the analogy to the eight-particle amplitude still further, we wish to compute the piece of $M_6^{T_A T_B T_C}$ that has a discontinuity in s_X. It is necessary, by the Steinmann relation, to consider only those terms that have $\lambda_B=\alpha_B-n$, where n is a non-negative integer, so that we have terms with no discontinuity in s_{15}. If we look at (5.10), we first sweep $C_{\lambda_B}^>$ to the left, picking up poles due to $\Gamma(\lambda_B-\alpha_B)$. The resulting contribution to $M_{6>}^{T_A T_B T_C}$ is given by

$$M_{6>}^{t_A t_B t_C}=\frac{(-s_1)^{\alpha_A}(-s_{15})^{\alpha_B}(-s_X)^{\alpha_C}}{2\pi i}$$

$$\times\sum_{n=0}^{\infty}\frac{(-1)^n}{n!}\int_{C_{\lambda_A}^>}d\lambda_A\Gamma(\lambda_A-\alpha_A)\Gamma(-\lambda_A)\Gamma(\alpha_B-\alpha_C-n)\Gamma(\lambda_A-\alpha_B+n)\Gamma(\alpha_B-\lambda_A+1-n)$$

$$\times(-\eta_{12})^{\lambda_A}(-\eta_{23})^{\lambda_B}\frac{\Gamma(\alpha_B+1)}{\Gamma(\alpha_B-\lambda_A+1)}\frac{b_>(\lambda_A;\alpha_B-n)}{\Gamma(\alpha_B-n+1)}. \tag{5.13}$$

In the above, we have written

$$\frac{\pi}{\sin\pi(\lambda_A-\lambda_B)}=\Gamma(\lambda_A-\lambda_B)\Gamma(\lambda_B-\lambda_A+1).$$

If we sweep $C_{\lambda_A}^>$ to the left, we pick up poles from $\Gamma(\lambda_A-\alpha_A)$. We can see from Figs. 13(c) and 13(d) that we also pick up poles from $\Gamma(\lambda_A-\alpha_B+n)$ due to a pinching of the $C_{\lambda_B}^>$ contour between the poles of $\Gamma(\lambda_B-\alpha_B)$ and $\pi/\sin\pi(\lambda_B-\lambda_A)$ [in order to visualize this, it may be helpful to imagine moving $C_{\lambda_A}^>$ and $C_{\lambda_B}^>$ to the left simultaneously in Figs. 13(c) and 13(d)]. These poles occur at $\lambda_A=\alpha_B-n$, α_B-n-1, $\alpha_B-n-2,\ldots,\alpha_B-m,\ldots$, where $m\geq n$. Note from Fig. 13(c) that $C_{\lambda_B}^>$ is not pinched between the poles at $\lambda_B=\alpha_B-n$ and at $\lambda_B=\lambda_A-1$, λ_A-2, etc. After some algebra, the pole expansion of (5.13) may be written

$$M_6^{\tau_A \tau_B \tau_C} = (-s_1)^{\alpha_A}(-s_{15})^{\alpha_B}(-s_X)^{\alpha_C}$$

$$\times \frac{(-\eta_{12})^{\alpha_A}(-\eta_{23})^{\alpha_B}}{\Gamma(-\alpha_B)} \sum_{m=0}^{\infty} \sum_{n=0}^{\infty} \frac{\Gamma(m-\alpha_A)\Gamma(\alpha_A-\alpha_B-m)}{m!} \frac{\Gamma(n-\alpha_B)\Gamma(\alpha_B-\alpha_C-n)}{n!}$$

$$\times \eta_{12}^{-m}\eta_{23}^{-n} b_>(\alpha_A-m;\alpha_B-n;\Phi_2)$$

$$+\frac{(-\eta_{12})^{\alpha_B}(-\eta_{23})^{\alpha_B}}{\Gamma(-\alpha_B)} \sum_{n=0}^{\infty} \sum_{m \geq n}^{\infty} \frac{\Gamma(m-\alpha_B)\Gamma(\alpha_B-\alpha_A-m)}{m!} \frac{\Gamma(n-\alpha_B)\Gamma(\alpha_B-\alpha_C-n)}{n!}$$

$$\times \eta_{12}^{-m}\eta_{23}^{-n} b_>(\alpha_B-m;\alpha_B-n;\Phi_2) \quad . \tag{5.14}$$

We pay special attention to the limits on the summation in the second term in (5.14). The restriction $m \geq n$ is directly due to the fact that in Fig. 13(c) the poles at $\lambda_B = \lambda_A, \lambda_A+1, \lambda_A+2$, etc., lie to the right of $C^>_{\lambda_B}$, while the poles of $\Gamma(\lambda_B - \alpha_B)$ lie to the left of $C^>_{\lambda_B}$.

We next turn our attention to $M_6^{\tau_A \tau_B \tau_C}$ in (5.9). If we sweep $C^<_{\lambda_A}$ to the left in Fig. 13(a), we obtain the following contribution from the poles of $\Gamma(\lambda_A - \alpha_B)$:

$$M_6^{\tau_A \tau_B \tau_C} = -\frac{(-s_1)^{\alpha_A}(-s_{15})^{\alpha_B}(-s_X)^{\alpha_C}}{2\pi i}$$

$$\times \sum_{m=0}^{\infty} \frac{(-1)^m}{m!} \int_{C^<_{\lambda_B}} d\lambda_B \Gamma(\alpha_B - \alpha_A - m)\Gamma(-\lambda_B)\Gamma(\lambda_B - \alpha_C)\Gamma(\lambda_B - \alpha_B + m + 1)\Gamma(\alpha_B - \lambda_B - n)$$

$$\times (-\eta'_{12})^{\alpha_B-m}(-\eta'_{23})^{\lambda_B} \frac{\Gamma(\alpha_B+1)}{\Gamma(\alpha_B-\lambda_B+1)} \frac{b_<(\alpha_B-m,\lambda_B;\Phi_2)}{\Gamma(\alpha_B-m+1)} . \tag{5.15}$$

We next sweep the $C^<_{\lambda_B}$ contour to the left in Fig. 13(b). The only poles that produce terms with a discontinuity in s_X come from the factor $\Gamma(\lambda_B - \alpha_B + m + 1)$, and occur at $\lambda_B = \alpha_B - m - 1$, $\alpha_B - m - 2$, $\alpha_B - m$ $-3, \ldots, \alpha_B - n, \ldots$, where $n \geq m + 1$. At these poles, the $C^<_{\lambda_A}$ contour in Fig. 13(a) is pinched between the poles of $\Gamma(\lambda_A - \alpha_B)$ and the poles of $\pi/\sin\pi(\lambda_A - \lambda_B)$ at $\lambda_A = \lambda_B + 1$, $\lambda_B + 2$, etc., in Eq. (5.9). We can complete the pole expansion of (5.15) and get

$$M_6^{\tau_A \tau_B \tau_C} = (-s_1)^{\alpha_A}(-s_{15})^{\alpha_B}(-s_X)^{\alpha_C} \frac{(-\eta'_{12})^{\alpha_B}(-\eta'_{23})^{\alpha_B}}{\Gamma(-\alpha_B)}$$

$$\times \sum_{m=0}^{\infty} \sum_{n \geq m+1}^{\infty} \frac{\Gamma(m-\alpha_B)\Gamma(\alpha_B-\alpha_A-m)}{m!} \frac{\Gamma(n-\alpha_B)\Gamma(\alpha_B-\alpha_C-n)}{n!}$$

$$\times (-\eta'_{12})^{-m}(-\eta'_{23})^{-n} b_<(\alpha_B-m;\alpha_B-n;\Phi_2). \tag{5.16}$$

If we examine the limits on the summation, we see that the condition $n \geq m + 1$ arises from the fact that in Fig. 13(a) the poles of $\Gamma(\lambda_A - \alpha_A)$ lie to the left of the contour $C^<_{\lambda_A}$, while the lowest pole of $\pi/\sin\pi(\lambda_A - \lambda_B)$ lying to the right of $C^<_{\lambda_A}$ occurs at $\lambda_A = \lambda_B + 1$. We remind the reader that the helicity contours have been carefully chosen in Figs. 13(a)–13(d) so that when the contours are closed to the right, the terms in Eq. (5.4) with $\lambda_A = \lambda_B$ are not counted twice. If we combine (5.14) and (5.15), we get the following pole expansion for $M_6^{\tau_A \tau_B \tau_C}$, for the piece with a discontinuity in s_X:

$$M_6^{\tau_A \tau_B \tau_C} = (-s_1)^{\alpha_A}(-s_{15})^{\alpha_B}(-s_X)^{\alpha_C}$$

$$\times \left[\frac{(-\eta_{12})^{\alpha_A}(-\eta_{23})^{\alpha_B}}{\Gamma(-\alpha_B)} \sum_{m=0}^{\infty} \sum_{n=0}^{\infty} \frac{\Gamma(m-\alpha_A)\Gamma(\alpha_A-\alpha_B-m)}{m!} \frac{\Gamma(n-\alpha_B-\alpha_C-m)}{n!} \right.$$

$$\times \eta_{12}^{-m}\eta_{23}^{-n} b_>(\alpha_A-m,\alpha_B-n;\Phi_2)$$

$$+\frac{(-\eta_{12})^{\alpha_B}(-\eta_{23})^{\alpha_B}}{\Gamma(-\alpha_B)} \sum_{m=0}^{\infty} \sum_{n=0}^{\infty} \frac{\Gamma(m-\alpha_B)\Gamma(\alpha_B-\alpha_A-m)}{m!} \frac{\Gamma(n-\alpha_B)\Gamma(\alpha_B-\alpha_C-n)}{n!}$$

$$\left. \times \eta_{12}^{-m}\eta_{23}^{-n} \bar{b}(\alpha_B-m,\alpha_B-n;\Phi_2) \right] . \tag{5.17}$$

We have defined the quantity

$$\bar{b}(\alpha_B-m;\alpha_B-n;\Phi_2) \equiv \theta(m-n)b_>(\alpha_B-m;\alpha_B-n;\Phi_2) + \theta(n-m+1)\Phi_2^{m-n} b_<(\alpha_B-m;\alpha_B-n;\Phi_2). \tag{5.18}$$

Let us now consider the multi-Regge limit of (5.16). We recall from (5.2) that in the multi-Regge limit, $\Phi_2 = 1$. If we assume factorization of the residues in (5.8) in the multi-Regge limit,[4,18] we then have that

$$b_>(\alpha_A - m; \alpha_B - n; \Phi_2 = 1) = \beta^A(t_A)\beta^{AB}(\alpha_A - m; t_A, t_B)\beta^{BC}(\alpha_B - n; t_B, t_C)\beta^C(t_C) , \tag{5.19}$$

$$\tilde{b}(\alpha_B - m; \alpha_B - n; \Phi_2 = 1) = \beta^A(t_A)\beta^{AB}(\alpha_B - m; t_A, t_B)\beta^{BC}(\alpha_B - n; t_B, t_C)\beta^C(t_C) . \tag{5.20}$$

In the multi-Regge limit, we may write (5.15) as

$$M_6^{T_A T_B T_C} = \beta^A(t_A)\beta^C(t_C)\Gamma(-\alpha_A)(-s_1)^{\alpha_A}\Gamma(-\alpha_B)(-s_{15})^{\alpha_B}\Gamma(-\alpha_C)(-s_X)^{\alpha_C}$$

$$\times \; [(-\eta_{12})^{\alpha_A}V_A(t_A, t_B; \eta_{12}) + (-\eta_{12})^{\alpha_B}V_B(t_A, t_B; \eta_{12})](-\eta_{23})^{\alpha_B}V_B(t_B; t_C; \eta_{23}) . \tag{5.21}$$

The standard double Reggeon-particle couplings[4,5,21] are defined by

$$V_A(t_A, t_B; \eta_{12}) = \frac{1}{\Gamma(-\alpha_A)\Gamma(-\alpha_B)} \sum_{m=0}^{\infty} \frac{\Gamma(m - \alpha_A)\Gamma(\alpha_A - \alpha_B - m)}{m!} \eta_{12}^{-m}\beta^{AB}(\alpha_A - m; t_A, t_B) ,$$

$$V_B(t_A, t_B; \eta_{12}) = \frac{1}{\Gamma(-\alpha_A)\Gamma(-\alpha_B)} \sum_{m=0}^{\infty} \frac{\Gamma(m - \alpha_B)\Gamma(\alpha_B - \alpha_A - m)}{m!} \eta_{12}^{-m}\beta^{AB}(\alpha_B - m; t_A, t_B) , \tag{5.22}$$

$$V_B(t_B, t_C; \eta_{23}) = \frac{1}{\Gamma(-\alpha_A)\Gamma(-\alpha_C)} \sum_{n=0}^{\infty} \frac{\Gamma(n - \alpha_B)\Gamma(\alpha_B - \alpha_C - n)}{n!} \eta_{23}^{-n}\beta^{BC}(\alpha_B - n; t_B, t_C) .$$

Let us temporarily turn our attention back to M_8. We wish to evaluate M_8 in the asymptotic limit appropriate to Fig. 1, in order to obtain the inclusive cross section given by Eq. (2.7). If the invariants have the behavior (3.37), then Eqs. (3.13)–(3.20) yield the following behavior for the group variables:

$$\chi_B \to i\infty, \quad \xi_A \to +i\infty, \quad \xi_C \to -i\infty, \quad \text{with } \omega_{AB}, \; \xi_B \text{ finite} . \tag{5.23}$$

If we restrict ourselves to the MFD, from (3.31) and (4.12) we get

$$\chi_E \to -i\infty, \quad \xi_D \to +i\infty, \quad \text{with } \omega_{DE}, \; \xi_E \text{ finite}. \tag{5.24}$$

It is evident from Figs. 10–12 that not only do the continuations of the polar angles ξ_A, ξ_C, and ξ_D become large, but also the continuations of the azimuthal angles χ_B and χ_E become large. From (3.11) and (3.20), we see that

$$\eta_{23}, \eta_{35} \to \infty . \tag{5.25}$$

Now in addition to the quantities in (5.1), we define the analogous quantities for Fig. 9(b), namely

$$\eta_{45}' \equiv \frac{s_{34}}{s_4 s_{25}}, \quad \eta_{35}' \equiv \frac{s_{45}}{s_X s_{34}}, \quad \Phi_5 \equiv \frac{\eta_{45}}{\eta_{45}'} = \frac{\eta_{23}'}{\eta_{23}} . \tag{5.26}$$

In the multi-Regge limit of M_8,

$$\eta_{45} = \eta_{45}', \quad \eta_{35} = \eta_{35}', \quad \Phi_5 = 1 . \tag{5.27}$$

In the HPRP limit of M_8, given by (5.23) and (5.24), the relations (5.2) and (5.5) break down. In par-

ticular, from Table VI we see that if we first continue to the MFD, then

$$\eta_{12}' = \eta_{45}' = m_\pi^2 / s_1 t_1 . \tag{5.28}$$

By examining Tables III and IV, it is apparent that even away from the MFD, η_{12}' and η_{45}' do not depend on ω_{AD} and ω_{DE} in the HPRP limit. As a result, any integral representation of M_8 that contributes to the inclusive cross section of Fig. 1 cannot involve the primed η's.[10] Finally, we note from (5.1) and (5.6) that in the HPRP limit, $\Phi_2 \to \infty$, $\Phi_5 \to \infty$.

Let us now consider in detail the analogous case of the HPRP limit of M_6, the six-particle amplitude of Fig. 8(a). The HPRP limit is given by (5.23). As noted in Ref. 10, the only representation of M_6 that contributes in the HPRP limit is that for $M_{6<}^{T_A T_B T_C}$ given in (5.7), since we have shown that the Steinmann relation implies $M_{6<}^{T_A T_B T_C}$ involves η_{12}' and η_{23}'.

Let us proceed to determine the asymptotic behavior of $M_{6>}^{T_A T_B T_C}$ in the HPRP limit. From (5.7), we see that the leading behavior as $\eta_{23} \to \infty$ is due to the leading singularity in the complex λ_B plane. This limit is then termed "mixed," for the leading singularities are Regge poles in J_A and J_C, and helicity poles in λ_B. From Fig. 13(c), we see that the leading singularity in λ_B that produces a term with a discontinuity in s_X results from a pinching of $C_{\lambda_B}^>$ against the "kinematic" pole at $\lambda_B = \alpha_B$. If we sweep back the contours in (5.7), we obtain a pole expansion analogous to (5.14); however, since $\eta_{23} \to \infty$ in the HPRP limit, the leading behavior is given by only the $n = 0$ terms, and we write

$$M_6^{\tau_A \tau_B \tau_C}(\text{HPRP}) = M_{6>}^{\tau_A \tau_B \tau_C}(\text{HPRP})$$

$$= (-s_1)^{\alpha_A}(-s_X)^{\alpha_C}\Gamma(\alpha_B - \alpha_C)$$

$$\times \left[(-\eta_{12})^{\alpha_A}\left(-\frac{s_2}{s_X}\right)^{\alpha_B} \sum_{m=0}^{\infty} \frac{\Gamma(m - \alpha_A)\Gamma(\alpha_A - \alpha_B - m)}{m!} \eta_{12}^{-m} b_>(\alpha_A - m, \alpha_B; \Phi_2 = \infty) \right.$$

$$\left. + (-\eta_{12})^{\alpha_B}\left(-\frac{s_2}{s_X}\right)^{\alpha_B} \sum_{m=0}^{\infty} \frac{\Gamma(m - \alpha_A)\Gamma(\alpha_B - \alpha_A - m)}{m!} \eta_{12}^{-m} b_>(\alpha_B - m; \alpha_B; \Phi_2 = \infty) \right]. \qquad (5.29)$$

In (5.29), we have denoted any possible Φ_2 dependence of the $b_>$'s. We note that we have no dependence to leading order on "small" invariants, such as s_{15}. Such dependence does not appear because we have kept only the leading term in η_{23}. On the other hand, since η_{12} is finite in the HPRP limit, it is necessary to keep all terms with $m \geq 0$.

Now let us take the HPRP limit of our multi-Regge expression for $M_6^{\tau_A \tau_B \tau_C}$, given by (5.17). Again, since $\eta_{23} \to \infty$, we keep only the $n = 0$ terms, so that (5.17) becomes

$$M_6^{\tau_A \tau_B \tau_C} = (-s_1)^{\alpha_A}(-s_X)^{\alpha_C}\Gamma(\alpha_B - \alpha_C)$$

$$\times \left[(-\eta_{12})^{\alpha_A}\left(-\frac{s_2}{s_X}\right)^{\alpha_B} \sum_{m=0}^{\infty} \frac{\Gamma(m - \alpha_A)\Gamma(\alpha_A - \alpha_B - m)}{m!} \eta_{12}^{-m} b_>(\alpha_A - m, \alpha_B; \Phi_2 = 1) \right.$$

$$\left. + (-\eta_{12})^{\alpha_B}\left(-\frac{s_2}{s_X}\right)^{\alpha_B} \sum_{m=0}^{\infty} \frac{\Gamma(m - \alpha_B)\Gamma(\alpha_B - \alpha_A - m)}{m!} \eta_{12}^{-m} \tilde{b}(\alpha_B - m; \alpha_B; \Phi_2 = 1) \right]. \qquad (5.30)$$

Since $m \geq 0$, we have from (5.18) that

$$\tilde{b}_>(\alpha_B - m, \alpha_B; \Phi_2 = 1) = b_>(\alpha_B - m, \alpha_B; \Phi_2 = 1). \qquad (5.31)$$

If we compare (5.29) and (5.30), then we see that the conditions for the identity of the couplings in the HPRP limit and in the multi-Regge limit are

$$b_>(\alpha_A - m, \alpha_B; \Phi_2 = 1) = b_>(\alpha_A - m, \alpha_B; \Phi_2 = \infty), \quad b_>(\alpha_B - m, \alpha_B; \Phi_2 = 1) = b_>(\alpha_B - m, \alpha_B; \Phi_2 = \infty). \qquad (5.32)$$

These will of course be satisfied if

$$b_>(\lambda_A, \lambda_B; \Phi_2 = 1) = b_>(\lambda_A, \lambda_B; \Phi_2 = \infty). \qquad (5.33)$$

The condition (5.33) is considerably more simple than those given in Ref. 10. This is due to two facts. First, we have carefully chosen the contours of integration in Figs. 13(a)–13(d) so that the terms in the partial-wave sum (5.3) with $\lambda_A = \lambda_B$ contribute to $M_{6>}^{\tau_A \tau_B \tau_C}$. This has the effect that when the contours are swept to the left, $M_{6<}^{\tau_A \tau_B \tau_C}$ is down by a power of η_{23}; the two terms are of the same order in the multi-Regge limit, but different order in the HPRP limit. Second, we have recognized that the identity of the two couplings is a statement that is true only to leading order in the large invariants. This is analogous to the case considered by DeTar and Weis[20] of the single-Reggeon couplings for the six-particle amplitude with a triple-Regge vertex in the dual resonance model.

From (5.19), (5.20), (5.31), and (5.32), we have

$$b_>(\alpha_A - m, \alpha_B; \Phi_2 = \infty) = \beta^A(t_A)\beta^{AB}(\alpha_A - m; t_A, t_B)\beta^{BC}(\alpha_B; t_B, t_C)\beta^C(t_C),$$

$$b_>(\alpha_B - m, \alpha_B; \Phi_2 = \infty) = \theta(m)\beta^A(t_A)\beta^{AB}(\alpha_B - m; t_A, t_B)\beta^{BC}(\alpha_B; t_B, t_C)\beta^C(t_C). \qquad (5.34)$$

Then in the HPRP limit, (5.30) becomes

$$M_6^{\tau_A \tau_B \tau_C} = \beta^A(t_A)\beta^C(t_C)\Gamma(-\alpha_A)(-s_1)^{\alpha_A}\Gamma(-\alpha_B)\left(-\frac{s_2}{s_X}\right)^{\alpha_B}(-s_X)^{\alpha_C}$$

$$\times \left[(-\eta_{12})^{\alpha_A}V_A(t_A, t_B; \eta_{12}) + (-\eta_{12})^{\alpha_B}V_B(t_A, t_B; \eta_{12}) \right]\Gamma(\alpha_B - \alpha_C)\beta^{BC}(\alpha_B; t_B, t_C). \qquad (5.35)$$

We remind the reader once again that the above is the piece of $M_6^{\tau_A \tau_B \tau_C}$ with a discontinuity in s_X. The discontinuity structure of (5.35) is identical with that of the five-particle amplitude of Fig. 5,[1,5,19] and hence is considerably more simple than that of the full six-particle amplitude.[18] To leading order in η_{23} in the HPRP limit, the two-Reggeon–particle coupling factors off, due to the assumed factorization of the residues of the linear six-particle amplitude in (5.19) and (5.20).

We now turn our attention back to M_8. In analogy to (5.4), we can break up the partial-wave sum in (4.18) so that the partial-wave amplitudes may be redefined in a singularity-free fashion. We let

$$M_{8\gg}^{T_A\cdots T_E} = \sum_{\lambda_B\geq\lambda_A=0}^{\infty}\sum_{J_A=\lambda_A}^{\infty}\sum_{J_B=\lambda_B}^{\infty}\sum_{\lambda_E\geq\lambda_D\geq0}^{\infty}\sum_{J_D=\lambda_D}^{\infty}\sum_{J_E=\lambda_E}^{\infty}\sum_{J_C=\lambda_B+\lambda_E}^{\infty}\eta_{12}^{\lambda_A}\eta_{23}^{\lambda_B}\eta_{45}^{\lambda_D}\eta_{35}^{\lambda_E}d_{0\lambda_A}^{\lambda_A}(\xi_A)d_{\lambda_A\lambda_B}^{J_B}\left(\xi_B+\frac{\pi}{2}\right)d_{0\lambda_D}^{J_D}(\xi_D)$$

$$\times d_{\lambda_D\lambda_E}^{J_E}(\xi_E+\pi/2)d_{0\lambda_C}^{J_C}(\xi_C+\pi/2)A_{\lambda_A\cdots\lambda_E}^{J_A\cdots J_E}(t_A\cdots\circ t_E)_{\gg}. \quad (5.36)$$

The double subscript "$\gg$" indicates that $\lambda_B\geq\lambda_A$ and $\lambda_E\geq\lambda_D$. Since we are only concerned with that part of M_8 with a discontinuity in s_X, we have set $\chi_C=0$; the loss of terms containing powers of η_{25} will not affect our results.

Now if, as in (5.8), we assume that the partial-wave amplitude has the J-plane poles

$$A_{\lambda_A\cdots\lambda_E}^{J_A\cdots J_E} = \frac{b_{\gg}(\lambda_A,\lambda_B,\lambda_D,\lambda_E;\Phi_2,\Phi_5)}{(J_A-\alpha_A)(J_B-\alpha_B)(J_C-\alpha_C)(J_D-\alpha_D)(J_E-\alpha_E)}, \quad (5.37)$$

we can write an integral representation for (5.36) similar to (5.7). If we then sweep back the angular momentum contours, we obtain the result

$$M_{8\gg}^{T_A\cdots T_E} = \frac{(-s_1)^{\alpha_A}(-s_{15})^{\alpha_B}(-s_X)^{\alpha_C}(-s_4)^{\alpha_D}(-s_{25})^{\alpha_E}}{(2\pi i)^4}$$

$$\times \int_{C_{\lambda_A}^>}d\lambda_A\int_{C_{\lambda_D}^>}d\lambda_D\int_{C_{\lambda_B}^>}d\lambda_B\int_{C_{\lambda_E}^>}d\lambda_E\frac{\Gamma(\lambda_A-\alpha_A)\Gamma(-\lambda_A)}{\Gamma(\alpha_B-\lambda_A+1)}\Gamma(\lambda_B-\alpha_B)\frac{\pi}{\sin\pi(\lambda_A-\lambda_B)}$$

$$\times\frac{\Gamma(\lambda_D-\alpha_D)\Gamma(-\lambda_D)}{\Gamma(\alpha_E-\lambda_D+1)}\Gamma(\lambda_E-\alpha_E)\frac{\pi}{\sin\pi(\lambda_D-\lambda_E)}$$

$$\times\Gamma(\lambda_B+\lambda_E-\alpha_C)\frac{\Gamma(\alpha_B+1)}{\Gamma(\lambda_B+1)}\frac{\Gamma(\alpha_E+1)}{\Gamma(\lambda_E+1)}(-\eta_{12})^{\lambda_A}(-\eta_{23})^{\lambda_B}$$

$$\times(-\eta_{45})^{\lambda_D}(-\eta_{35})^{\lambda_E}b_{\gg}(\lambda_A,\lambda_B,\lambda_D,\lambda_E;\Phi_2,\Phi_5). \quad (5.38)$$

The helicity contours C_{λ_A}, C_{λ_D}, C_{λ_B}, and C_{λ_E} are shown in Figs. 14(a)–14(d); they are drawn so that the sum in (5.36) will be reproduced when all the contours are closed to the right. We can sweep the helicity contours to the left, and in Table IX, we give the pole expansion of (5.38) for the terms that have a discontinuity in s_X.

We can define the continuations of the following sums, in addition to that of (5.36):

$$M_{8<>}^{T_A\cdots T_E} \sim \sum_{\lambda_A>\lambda_B\geq0}^{\infty}\sum_{J_A=\lambda_A}^{\infty}\sum_{J_B=\lambda_B}^{\infty}\sum_{\lambda_E\geq\lambda_D\geq0}^{\infty}\sum_{J_D=\lambda_D}^{\infty}\sum_{J_E=\lambda_E}^{\infty}\sum_{J_C=\lambda_B+\lambda_E}^{\infty},$$

$$M_{8><}^{T_A\cdots T_E} \sim \sum_{\lambda_B\geq\lambda_A\geq0}^{\infty}\sum_{J_A=\lambda_A}^{\infty}\sum_{J_B=\lambda_B}^{\infty}\sum_{\lambda_D>\lambda_E\geq0}^{\infty}\sum_{J_D=\lambda_D}^{\infty}\sum_{J_E=\lambda_E}^{\infty}\sum_{J_C=\lambda_B+\lambda_E}^{\infty},$$

$$M_{8<<}^{T_A\cdots T_E} \sim \sum_{\lambda_A>\lambda_B\geq0}^{\infty}\sum_{J_A=\lambda_A}^{\infty}\sum_{J_B=\lambda_B}^{\infty}\sum_{\lambda_D>\lambda_E\geq0}^{\infty}\sum_{J_D=\lambda_D}^{\infty}\sum_{J_E=\lambda_E}^{\infty}\sum_{J_C=\lambda_B+\lambda_E}^{\infty}.$$

Now as in the case of M_6, from (5.28) the only sum that has an integral representation that remains valid in terms of the O(3) variables in the HPRP limit is $M_{8\gg}^{T_A\cdots T_E}$. In addition, the only continuation that contributes to leading order in η_{23} and η_{35} in the HPRP limit is again that of $M_{8\gg}^{T_A\cdots T_E}$. From (5.25), the leading contribution comes from those terms in Table IX with $n=w=0$. As in the discussion of M_6, our conditions for the identity of the couplings in the multi-Regge and the HPRP limit are

$$b_{\gg}(\alpha_A-m,\alpha_B,\alpha_D-v,\alpha_E;\Phi_2=\Phi_5=1)=b_{\gg}(\alpha_A-m,\alpha_B,\alpha_D-v,\alpha_E;\Phi_2=\Phi_5=\infty),\text{ etc.}$$

The above, and three similar conditions will be satisfied if

$$b_{\gg}(\lambda_A,\lambda_B,\lambda_D,\lambda_E;\Phi_2=\Phi_5=1)=b_{\gg}(\lambda_A,\lambda_B,\lambda_D,\lambda_E;\Phi_2=\Phi_5=\infty). \quad (5.39)$$

The above clearly corresponds to (5.33). Let us again assume that in the multi-Regge limit, residues as in (5.37) factorize according to relations similar to (5.19) and (5.20), e.g.,

$$b_{\gg}(\alpha_A-m,\alpha_B-n,\alpha_D-v,\alpha_E-w;\Phi_2=\Phi_5=1)$$

$$=\beta^A(t_A)\beta^{AB}(\alpha_A-m;t_A,t_B)\beta^D(t_D)\beta^{DE}(\alpha_D-v;t_D,t_E)\beta^{BEC}(\alpha_B-n,\alpha_E-w;t_B,t_E,t_C)\beta^C(t_C). \quad (5.40)$$

In the HPRP limit, to leading order in η_{23} and η_{35}, we have that

$$M_8^{\tau_A \cdots \tau_E} = \beta^A(t_A)\beta^D(t_D)\Gamma(-\alpha_A)(-s_1)^{\alpha_A}\Gamma(-\alpha_B)\left(-\frac{s_2}{s_X}\right)^{\alpha_B}(-s_X)^{\alpha_C}\Gamma(-\alpha_D)(-s_4)^{\alpha_D}\Gamma(-\alpha_E)\left(-\frac{s_5}{s_X}\right)^{\alpha_E}$$

$$\times [(-\eta_{12})^{\alpha_A}V_A(t_A,t_B;\eta_{12}) + (-\eta_{12})^{\alpha_B}V_B(t_A,t_B;\eta_{12})]$$

$$\times [(-\eta_{45})^{\alpha_D}V_D(t_D,t_E;\eta_{45}) + (-\eta_{45})^{\alpha_E}V_E(t_D,t_E;\eta_{45})]$$

$$\times \Gamma(\alpha_B + \alpha_E - \alpha_C)\beta^{BEC}(\alpha_B,\alpha_E;t_B,t_E,t_C)\beta^C(t_C). \tag{5.41}$$

Notice that in (5.41), the square brackets contain the ordinary double-Regge couplings[1,5,19] such as those that appear in the five-particle amplitude of Fig. 5. The new feature in (5.41) is the triple-Regge residue

$$\beta^{BEC}(\alpha_B,\alpha_E;t_B,t_E,t_C) = \beta(p=0,\alpha_B,\alpha_E;t_B,t_E,t_C). \tag{5.42}$$

The expression appearing in the right-hand side of (5.42) is the $p=n=w=0$ term in the pole expansion of the triple-Regge coupling in the scheme of Weis.[4,5,21] The full expansion is given by

$$V_{BE} = \frac{1}{\Gamma(-\alpha_B)\Gamma(-\alpha_C)\Gamma(-\alpha_E)} \sum_{n,w,p=0}^{\infty} \frac{\Gamma(n+p-\alpha_B)\Gamma(w+p-\alpha_E)\Gamma(\alpha_B+\alpha_E-\alpha_C-n-w-2p)}{n!w!p!}$$

$$\times \eta_{23}^{-n}\eta_{35}^{-w}\left(\frac{\eta_{23}\eta_{35}}{\eta_{25}}\right)^{-p}\beta(p,\alpha_B-n-p,\alpha_E-w-p;t_B,t_E,t_C). \tag{5.43}$$

From (5.25) we expect that only the $n=w=p$ term survives in the HPRP limit (we might also add that $\eta_{25}=0$ in the MFD). As in the case of M_6, we see that if the couplings have the trivial Φ_2 and Φ_5 dependence of (5.39), the multi-Regge and HPRP limits are equivalent to leading order in η_{23} and η_{35}.

Having established the connection between the multi-Regge and the HPRP limit, we now wish to develop an intuitive picture of the latter. In Sec. VI we will do so, and show the plausibility of (5.39). In addition, we will show the connection between (5.39) and the commutativity of the limits.
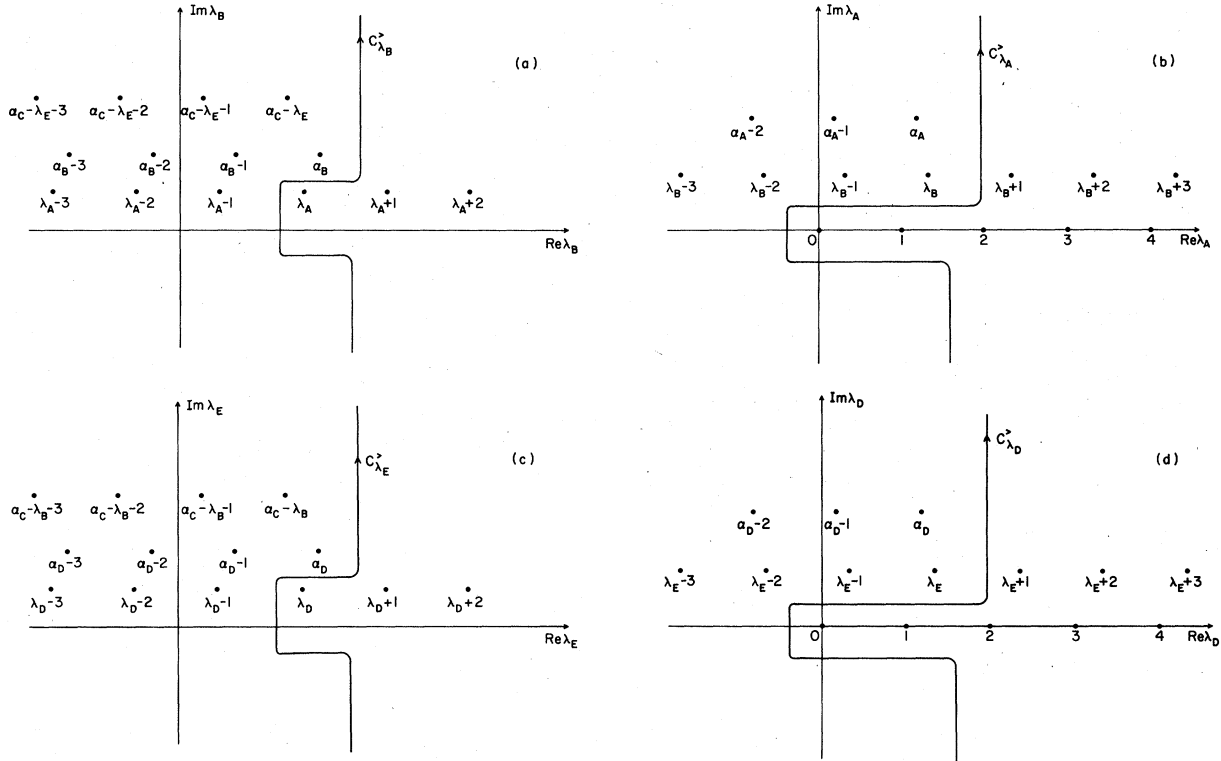

FIG. 14. Helicity contours used to define $M_8^{\tau_A \cdots \tau_E}$. All contours are chosen so as to reproduce the partial-wave sum for $\lambda_B \geq \lambda_A$ and $\lambda_E \geq \lambda_D$.

TABLE IX. Helicity-pole expansion of $M_{8\gg}^{T_A\cdots T_E}$.

$$
M_{8\gg}^{T_A\cdots T_E} = \frac{(-s)^{\alpha_A}(-s_X)^{\alpha_C}(-s_4)^{\alpha_D}}{\Gamma(-\alpha_B)\Gamma(-\alpha_E)} \left(-\frac{s_2}{s_X}\right)^{\alpha_B} \left(-\frac{s_5}{s_X}\right)^{\alpha_E}
$$

$$
\times \sum_{n=0}^{\infty} \sum_{w=0}^{\infty} \frac{\Gamma(n-\alpha_B)}{m!} \eta_{23}^{-n} \frac{\Gamma(w-\alpha_E)}{w!} \eta_{35}^{-w} \Gamma(\alpha_B + \alpha_E - \alpha_C - n - w)
$$

$$
\times \left[(-\eta_{12})^{\alpha_A}(-\eta_{45})^{\alpha_D} \sum_{m=0}^{\infty}\sum_{v=0}^{\infty} \frac{\Gamma(m-\alpha_A)\Gamma(\alpha_A-\alpha_B-m)}{m!}\eta_{12}^{-m} \frac{\Gamma(v-\alpha_D)\Gamma(\alpha_D-\alpha_E-v)}{v!}\eta_{45}^{-v} \right.
$$

$$
\times b_{\gg}(\alpha_A - m, \alpha_B - n, \alpha_D - v, \alpha_E - w; \Phi_2, \Phi_5)
$$

$$
+ (-\eta_{12})^{\alpha_B}(-\eta_{45})^{\alpha_D} \sum_{m\geq n}\sum_{v=0}^{\infty} \frac{\Gamma(m-\alpha_B)\Gamma(\alpha_B-\alpha_A-m)}{m!}\eta_{12}^{-m} \frac{\Gamma(v-\alpha_D)\Gamma(\alpha_D-\alpha_E-v)}{v!}\eta_{45}^{-v}
$$

$$
\times b_{\gg}(\alpha_B - m, \alpha_B - n, \alpha_D - v, \alpha_E - w; \Phi_2, \Phi_5)
$$

$$
+ (-\eta_{12})^{\alpha_A}(-\eta_{45})^{\alpha_E} \sum_{m=0}^{\infty}\sum_{v\geq w} \frac{\Gamma(m-\alpha_A)\Gamma(\alpha_A-\alpha_B-m)}{m!}\eta_{12}^{-m} \frac{\Gamma(v-\alpha_E)\Gamma(\alpha_E-\alpha_D-v)}{v!}\eta_{45}^{-v}
$$

$$
\times b_{\gg}(\alpha_A - m, \alpha_B - n, \alpha_E - v, \alpha_E - w; \Phi_2, \Phi_5)
$$

$$
+ (-\eta_{12})^{\alpha_B}(-\eta_{45})^{\alpha_E} \sum_{m\geq n}\sum_{v\geq w} \frac{\Gamma(m-\alpha_B)\Gamma(\alpha_B-\alpha_A-m)}{m!}\eta_{12}^{-m} \frac{\Gamma(v-\alpha_E)\Gamma(\alpha_E-\alpha_D-v)}{v!}\eta_{45}^{-v}
$$

$$
\left. \times b_{\gg}(\alpha_B - m, \alpha_B - n, \alpha_E - v, \alpha_E - w, \Phi_2, \Phi_5) \right]
$$

VI. INTERPRETATION OF THE HPRP LIMIT

In order to gain some insight into Eq. (5.41), we shall consider the behavior of the O(3) variables as we approach the MFD. For definiteness, let us consider the following limit of M_8, where the limit is determined by the invariants, as opposed to the group variables:

$$
s_{12}, s_1, s_2, s_X, s_2/s_X \to \infty,
$$

$$
s_{45}, s_4, s_5, s_5/s_X, \tag{6.1}
$$

$$
t_1, t_2, t_3, t_4, t_5, \eta_{12}, \eta_{45} \text{ fixed}.
$$

In analogy to the case of the six-particle amplitude considered by Jones, Low, and Young,[22] the limit (6.1) does not uniquely determine the asymptotic behavior of the group variables. However, the different group-theoretic limits consistent with (6.1) give rise to different types of power-law behavior in the invariants. Now from the discussion of Secs. II and III, the limit of interest of the O(3) variables in the HPRP limit is the following:

$$
\xi_A \to +i\infty, \quad \xi_C \to -i\infty, \quad \xi_D \to -i\infty,
$$

$$
\chi_B \to -i\infty, \quad \chi_E \to -i\infty, \tag{6.2}
$$

$$
\omega_{AB}, \omega_{DE}, \xi_B, \xi_E \text{ finite}.
$$

Although other limits of the O(3) variables are also implied by (6.1), we see from our result (5.41) that the limit (6.2) gives rise to an expres-

sion with a discontinuity in s_X. The expression (5.41) bears a strong resemblance (to within multiplicative terms) to the multi-Regge expansion of the amplitude in Fig. 5.[1,4,5] This resemblance becomes more remarkable when we recall from the end of Sec. II that in the MFD, the SO(2,1) parametrization of M_8 becomes identical to that of a set of "naive" momenta given by (3.41). Since this latter parametrization is identical to that of a five-particle amplitude given by (3.40), it is not surprising that (5.41) contains factors corresponding to the product of two five-particle amplitudes. In fact, from Eq. (3.42), it does seem surprising that helicity poles, rather than Regge poles, would control the asymptotic behavior of the inclusive cross section in χ_2 and χ_5 (or equivalently $i\chi_B$ and $i\chi_E$). It is inviting to take a closer look at the O(3) parametrization of M_8 as we approach the MFD. For our purposes, we will regard the MFD as the following submanifold of the O(3) parameters:

$$
\text{MFD:} \quad t_A = t_D, \quad t_B = t_E, \quad t_C = 0,
$$

$$
\xi_B = \xi_E = 0, \quad \xi_A = -\xi_D, \quad \chi_B = \chi_E. \tag{6.3}
$$

It will become apparent that conditions such as (5.37) that guarantee the identity of the double-Regge couplings in the HPRP limit and the multi-Regge limit, in addition to their obvious simplicity, are suggested by the kinematics in the MFD.

First of all, let us consider the invariants η_{12}

and η_{45} associated with the double-Regge vertices. Now in Sec. V, we showed that (5.41) is identical with the result obtained by taking the limit (6.1) of the multi-Regge expansion of M_8. It is important to realize, however, that the kinematic relations for η_{12} and η_{45} such as (3.19) break down in the MFD and instead are replaced by (3.36). In terms of the O(3) variables we have

$$\eta_{12} = \frac{m_\pi^2 - t_A - t_B + 2(t_A t_B)^{1/2} \cos\omega_{AB}}{\lambda(m_\pi^2, t_A, t_B)} \to \eta_{12}$$

$$= \frac{m_\pi^2 - t_A - t_B + 2(t_A t_B)^{1/2} \sin\omega_{AB}}{\lambda(m_\pi^2, t_A, t_B)} \quad (6.4)$$

and a similar relation for η_{45}. As a result of (6.4), if one wishes to continue (5.41) from an arbitrary point in the HPRP limit to the MFD, it is necessary to express (5.41) entirely in terms of invariants, and use that form when performing the continuation (the continuation is, of course, trivial). Once in the MFD, one may reexpress the invariants in terms of the group variables using (6.4). The physical significance of (6.4) can be seen from (3.36) and (3.42). The correct form of M_8 in the MFD and in the HPRP limit (6.2) can be obtained by expressing (5.41) in terms of the O(3) variables, continuing to the MFD, and making the extra substitution

$$\omega_{AB}, \omega_{DE} \to \omega_N , \quad (6.5)$$

where ω_N is the Toller angle at the double-Regge vertex for the naive momentum set of Fig. 1. We remind the reader that the contribution of the O(3) variables in the HPRP limit is given by the SO(2,1) expansion, so that (6.5) follows directly from (3.42).

Let us consider the behavior of the other O(3) variables as we gradually approach the MFD. If we set $\chi_C = 0$, then from Table VII and Table VIII, we have

$$p_C^{F_C} = [\tfrac{1}{2}\sqrt{t_C}, -(t_C/4 - m_N^2)^{1/2} \sin(\xi_C + \pi/2),$$

$$0, -(t_C/4 - m_N^2)^{1/2} \cos(\xi_C + \pi/2)] . \quad (6.6)$$

Since

$$p_C^{F_B} = B_z(-\theta_B) p_C^{F_C} , \quad (6.7)$$

we have that (writing $p_C^{F_B}$ as a column vector)

$$p_C^{F_B} = \begin{bmatrix} \tfrac{1}{2}\sqrt{t_C}\cosh\theta_B + \left(\dfrac{t_C}{4} - m_N^2\right)^{1/2} \cos\left(\xi_C + \dfrac{\pi}{2}\right)\sinh\theta_B \\[2ex] -\left(\dfrac{t_C}{4} - m_N^2\right)^{1/2} \sin\left(\xi_C + \dfrac{\pi}{2}\right) \\[2ex] 0 \\[2ex] -\tfrac{1}{2}\sqrt{t_C}\sinh\theta_B - \left(\dfrac{t_C}{4} - m_N^2\right)^{1/2} \cos\left(\xi_C + \dfrac{\pi}{2}\right)\cosh\theta_B \end{bmatrix} .$$
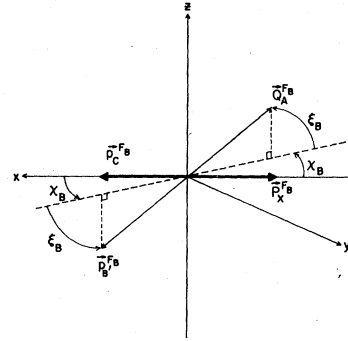
$$(6.8)$$

FIG. 15. Orientation of vectors in the F_B frame after continuation to $t_B = t_E$ and $t_C = 0$. Note that $P_x = Q_B - P_C$.

From (4.7), when $t_B = t_E$, we have

$$\cosh\theta_B = \frac{1}{2}\left(\frac{t_C}{t_B}\right)^{1/2} , \quad \sinh\theta_B = \left(\frac{t_B - 4t_B}{4t_B}\right)^{1/2} . \quad (6.9)$$

If we continue t_C from the upper half-plane to the real axis below the threshold at $t = 4m_N^2$, at $t = 0$ we have that

$$p_C^{F_B} = [-m_N \cos(\xi_C + \pi/2), im_N \sin(\xi_C + \pi/2), 0, 0] . \quad (6.10)$$

From Table VI and Eq. (4.12), we have

$$\sin\xi_C = \frac{t_B + m_N^2 - s_X}{2m_N\sqrt{t_B}} . \quad (6.11)$$

The Eq. (6.10) becomes

$$p_C^{F_B} = \left[\frac{t_B + m_N^2 - s_X}{2\sqrt{t_B}} , \frac{\lambda^{1/2}(t_B, m_N^2, s_X)}{2\sqrt{t_B}}, 0, 0\right] . \quad (6.12)$$

In Fig. 15, we show the orientations of the various momenta in the F_B frame when we continue to the manifold $t_B = t_E$, and $t_C = 0$. Let us consider what happens when we impose the condition $\xi_B = 0$ found in (6.3). This last restriction causes χ_B to become a polar angle, defining the angle that the vector $\vec{p}_B^{F_B}$ makes with respect to a new z axis defined by $\vec{p}_C^{F_B}$. Let us define a new submanifold of O(3) parameters, which we call R. We define R by

$$R: \quad t_B = t_E, \quad t_C = 0, \quad \text{and} \quad \xi_B = \xi_E = 0 , \quad (6.13)$$

so that R contains the MFD given by (6.3). The previous discussion suggests that if we continue to the submanifold R, and rotate from the F_B frame to a frame such that $\vec{p}_C$ lies along the z axis, then our original O(3) expansion is such that the behavior of M_8 as $\cos\chi_B \to \infty$ is governed by singularities in the angular momentum of the $p_A p_{A'} p_B$ system, that is, J_B. To summarize this kinematic result, we state that on the submanifold R, the independent azimuthal angles χ_B and

χ_E associated with the triple-Regge vertex become ordinary polar angles of the type that give rise to Regge behavior.

Let us now consider what happens to the partial-wave expansion (4.17) when we approach R. If we set $\chi_C = 0$ and let $\xi_B = \xi_E = 0$, we have

$$M_8 = \sum_{\lambda_A = -\infty}^{+\infty} \sum_{J_A = J_B = |\lambda_A|}^{\infty} \sum_{\lambda_B = -J_B}^{+J_B} \sum_{\lambda_D = -\infty}^{+\infty} \sum_{J_D, J_E = |\lambda_D|}^{\infty} \sum_{\lambda_E = -J_E}^{+J_E} \sum_{J_C = |\lambda_B + \lambda_E|}^{\infty} \sum_{\lambda_C = -J_C}^{+J_C}$$

$$\times e^{i\lambda_A \omega_{AB}} e^{i\lambda_B \chi_B} e^{i\lambda_D \omega_{DE}} e^{i\lambda_E \chi_E} d_{0\lambda_A}^{J_A}(\xi_A) d_{\lambda_A \lambda_B}^{J_B}(\pi/2) d_{0\lambda_D}^{J_D}(\xi_D) d_{\lambda_D \lambda_E}^{J_E}(\pi/2) d_{\lambda_C 0}^{J_C}(\xi_C + \pi/2) A_{\lambda_A \cdots \lambda_B}^{J_A \cdots J_E}(t_A \cdots t_E).$$

(6.14)

In (6.14), the terms are zero unless $\lambda_B + \lambda_E + \lambda_C = 0$. Now we may recombine the d functions in the following fashion:

$$\sum_{\lambda_B = -J_B}^{+J_B} d_{\lambda_A \lambda_B}^{J_B}(\pi/2) e^{i\lambda_B \chi_B} d_{\lambda_B \lambda_B}^{J_B}(-\pi/2) = \langle J_B, \lambda_A | R_y(\pi/2) R_z(-\chi_B) R_y(-\pi/2) | J_B, \nu_B \rangle$$

$$= \langle J_B, \lambda_A | R_z(\pi/2) R_y(\chi_B) R_z(-\pi/2) | J_B, \nu_B \rangle$$

$$= e^{-i\lambda_A \pi/2} d_{\lambda_A \nu_B}^{J_B}(\chi_B) e^{i\nu_B \pi/2},$$

(6.15)

and similarly

$$\sum_{\lambda_E = -J_E}^{+J_E} d_{\lambda_D \lambda_E}^{J_E}(\pi/2) e^{i\lambda_E \chi_E} d_{\lambda_E \nu_E}^{J_E}(-\pi/2) = e^{-i\lambda_D \pi/2} d_{\lambda_D \nu_E}^{J_E}(\chi_E) e^{i\nu_E \pi/2}.$$

(6.16)

Then

$$M_8 = \sum_{\lambda_A = -\infty}^{+\infty} \sum_{J_A, J_B = |\lambda_A|}^{\infty} \sum_{\nu_B = -J_B}^{+J_B} \sum_{\lambda_D = -\infty}^{+\infty} \sum_{J_D, J_E = |\lambda_D|}^{\infty} \sum_{\nu_E = -J_E}^{+J_E} \sum_{\lambda_C = -J_B - J_E}^{J_B + J_E} \sum_{J_C = |\lambda_C|}^{\infty}$$

$$\times e^{i\lambda_A(\omega_{AB} - \pi/2)} e^{i\lambda_D(\omega_{DE} - \pi/2)} d_{0\lambda_A}^{J_A}(\xi_A) d_{\lambda_A \nu_B}^{J_B}(\chi_B) d_{\lambda_C 0}^{J_C}(\xi_C + \pi/2) d_{0\lambda_D}^{J_D}(\xi_D) d_{\lambda_D \nu_E}^{J_E}(\chi_E) B_{\lambda_A \nu_B \lambda_C \lambda_D \nu_E}^{J_A \cdots J_E}(t_A \cdots t_E);$$

(6.17)

In the last equation we introduced the quantity

$$B_{\lambda_A \nu_B \lambda_C \lambda_D \nu_E}^{J_A \cdots J_E} = e^{(i\pi/2)\nu_B} e^{(i\pi/2)\nu_E} \sum_{\lambda_B = -J_B}^{+J_B} \sum_{\lambda_E = -J_E}^{+J_E} d_{\nu_B \lambda_B}^{J_B}(\pi/2) d_{\nu_E \lambda_E}^{J_E}(\pi/2) A_{\lambda_A \lambda_B \lambda_C \lambda_D \lambda_E}^{J_A \cdots J_E}.$$

(6.18)

Now since (6.18) is just a linear combination of partial-wave amplitudes,

$$B_{\lambda_A \nu_B \lambda_C \lambda_D \nu_E}^{J_A \cdots J_E}$$

has poles at $J_A = \alpha_A$, $J_B = \alpha_B$, etc. It would appear that the asymptotic behavior of M_8 in χ_B and χ_E is governed by Regge poles rather than helicity poles. We caution the reader that this last observation is merely qualitative, due to the complicated helicity structure of (6.18). In order to make these arguments rigorous, it is necessary to reexpress (6.17) in such a fashion that all kinematic singularities in helicity are displayed, as in (5.38).[5,6,19] We expect that such a procedure can be found, since (6.17) must have the same asymptotic behavior as (6.14).

Having seen that both Fig. 15 and Eq. (6.17) suggest a purely "Regge" interpretation of the helicity singularities in λ_B and λ_E, let us pursue the Regge analogy further. Consider the angles

$$\omega_{AB}^N = \omega_{AB} - \pi/2, \quad \omega_{DE}^N = \omega_{DE} - \pi/2.$$

(6.19)

If we continue to the submanifold R, then from exactly the same arguments as those leading to (3.42), we have that ω_{AB}^N and ω_{DE}^N correspond to the Toller angles at the double-Regge vertices for the "naive" sets of momenta shown in Figs. 16(a) and
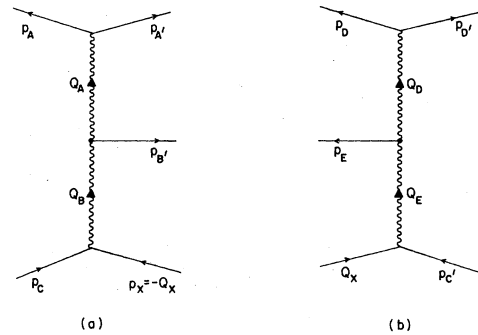

FIG. 16. Diagrams corresponding to the O(3) parametrization of "naive" sets of momenta that result on continuation to the submanifold R.

16(b). We see that ω_{AB}^N and ω_{DE}^N are precisely the angles that appear in (6.17). From (6.4), we see that if it is possible to rigorously take the limit (6.2) of (6.17), the correct dependence on the O(3) variables will be obtained quite naturally. From both the kinematics of Fig. 15 and the partial-wave sum (6.17), it appears that the question of whether the double-Regge couplings in the HPRP limit are identical with those in the multi-Regge limit is related to the question of whether or not the limits may be approached in any fashion. In particular,

if we can rigorously continue to R and then take the limit (6.2), the O(3) parametrization itself "factorizes" into two pieces appropriate to 16(a) and 16(b).

Now that we have developed an intuitive understanding of the HPRP limit and related our group parameters to physical quantities in the reaction of Fig. 1, all that remains is to completely specify (5.41) in terms of measured quantities. In Sec. VII, we will show that the Regge residues are fixed by unitarity and factorization.

VII. DETERMINATION OF THE RESIDUES

In order to determine the residues in (5.41), we will return to the SO(2, 1) notation of Sec. III so that our final result can be easily compared with the exclusive Deck model of Ref. 1. We then let $t_A \to t_1$, $\alpha_A \to \alpha_1$, etc. Now (5.41) corresponds to a signatured amplitude containing only right-hand cuts in the large invariants, so that the full amplitude is obtained by summing over the allowed cuts.[23] If we perform such a summation, the final result, to leading order in η_{23} and η_{35}, may be expressed neatly in terms of the factorized quantities of Weis[21]:

$$\mathrm{disc}_{s_X} M_8 = \beta_1(t_1)\Gamma(-\alpha_1)\Gamma(-\alpha_2)[\xi_1\xi_{21}s_1^{\alpha_1}s_{15}^{\alpha_2}\eta_{12}^{\alpha_1}\eta_{23}^{\alpha_2}V_1(t_1,t_2;\eta_{12}) + \xi_2\xi_{21}s_1^{\alpha_1}s_{15}^{\alpha_2}\eta_{12}^{\alpha_2}\eta_{23}^{\alpha_2}V_2(t_1,t;\eta_{12})]$$

$$\times \beta_4(t_4)\Gamma(-\alpha_4)\Gamma(-\alpha_5)[\xi_4\xi_{54}s_4^{\alpha_4}s_{24}^{\alpha_5}\eta_{45}^{\alpha_4}\eta_{35}^{\alpha_5}V_4(t_4,t_5;\eta_{45}) + \xi_5\xi_{45}s_4^{\alpha_4}s_{24}^{\alpha_5}\eta_{45}^{\alpha_5}\eta_{35}^{\alpha_5}V_5(t_4,t_5;\eta_{45})]$$

$$\times \beta_3(t_3)\frac{2\pi i}{\Gamma(\alpha_3+1)}s_X^{\alpha_3}\frac{\sin\pi(\alpha_3-\alpha_2-\alpha_5)}{\sin\pi\alpha_3}V_{25}.\tag{7.1}$$

The signature factors ξ_i, ξ_{ij} give the phase of the amplitude in terms of the trajectories α_i and the singularities τ_i. For the terms in the first bracket of (7.1), we have $\xi_i = e^{-i\pi\alpha_i}+\tau_i$, $\xi_{ij} = e^{-i\pi(\alpha_i-\alpha_j)}+\tau_i\tau_j$, etc., but for the terms in the second bracket, we have $\xi_i = e^{+i\pi\alpha_i}+\tau_i$, $\xi_{ij} = e^{+i\pi(\alpha_i-\alpha_j)}+\tau_i\tau_j$, etc. This is due to the fact that M_8 is evaluated above the cuts in the subenergies of Fig. 8(a), and below the cuts in the subenergies of Fig. 8(b) (Refs. 12 and 24) (note that since we are taking the discontinuity in s_X, we must evaluate M_8 both above and below the cut). We also remind the reader that $V_{25} = V_{DE}$ is the general triple-Regge coupling appearing in (5.43); in the HPRP limit, we only keep the $n=w=p=0$ term. Now in the MFD in the HPRP limit, we have

$$\mathrm{disc}_{s_X} M_8 = 2i[\beta_1(t_1)\Gamma(-\alpha_2)]^2|\xi_1\xi_{21}s_2^{\alpha_2-\alpha_1}s_{12}^{\alpha_1}V_1(t_1,t_2;\eta_{12}) + \xi_2\xi_{12}s_1^{\alpha_1-\alpha_2}s_{12}^{\alpha_2}V_2(t_1,t_2;\eta_{12})|^2$$

$$\times \beta_3(0)s_X^{\alpha_3-2\alpha_2}f(0,t_2,t_2).\tag{7.2}$$

In the above, $f(0,t_2,t_2)$ is a standard form for the triple-Regge coupling [see Eq. (6.39) of Ref. 4]. Note that (7.2) represents the contribution to $\mathrm{disc}_{s_X}M_8$ from a particular set of poles $\alpha_1\cdots\alpha_5$ for the special case $\alpha_1 = \alpha_4$ and $\alpha_2 = \alpha_5$. As in the case of the exclusive Deck model,[1,25] the pion and Pomeron trajectories dominate, so that $\alpha_1 = \alpha_4 = \alpha_\pi$ and $\alpha_2 = \alpha_5 = \alpha_P$.

Now as we have discussed in Sec. V, and made plausible in Sec. VI, if the Reggeon-particle couplings have the trivial Φ_2, Φ_5 dependence of (5.39), the double-Regge couplings $V_1(t_1,t_2;\eta_{12})$ and $V_2(t_1,t_2;\eta_{12})$ appearing in (7.2) are, to leading order in the HPRP limit, given by (2.13) and (2.14). From Ref. 1 we have

$$P(t_1,t_2) = \tfrac{1}{2}\beta_{\pi P\pi}(t_2),\tag{7.3}$$

where $\beta_{\pi P\pi}(t_2)$ is the pion-Pomeron-pion single-Regge coupling.

The function $M(t_1,t_2)$ necessary to guarantee the convergence of the hypergeometric series in (2.13) and (2.14) is now given by

$$M(t_1,t_2) = \frac{s_{12}}{s_1 s_{2\max}(s_{12},s_1,s_X,t_2)},\tag{7.4}$$

where in terms of the quantities in (2.5),

$$s_{2\max} = \bar{s}_X + m_\pi^2 + 2q_{20}^M q_0^M$$
$$+ 2|\vec{q}_2^M||\vec{q}^M|(\cos\theta_1\cos\psi_2 + \sin\theta_1\sin\psi_2).\tag{7.5}$$

In the HPRP limit, since $s_1/s_{12} \to 0$, and $s_X/s_2 \to 0$, we have

$$M(t_1,t_2) = [m_\pi^2 - t_1 - t_2 + 2(t_1t_2)]^{-1}.\tag{7.6}$$

As described in Ref. 1, $M(t_1, t_2)/\eta_{12} \lesssim 1$ in the physical region of the reaction, so that $V_1(t_1, t_2; \eta_{12})$ and $V_2(t_1, t_2; \eta_{12})$ are free of cuts in η_{12}. We note that due to (7.4), our double-Regge couplings are slightly different from the exclusive case,[1] but by (7.6) they agree to leading order in the HPRP limit, as we desire.

Now if we recall that M_5, the five-particle amplitude for the reaction of Fig. 5, is given by $M_5 = H_1 + H_2$, where H_1 and H_2 are given by (2.11) and (2.12), then we may rewrite the contribution to $\mathrm{disc}_{s_X} M_8$ from a particular trajectory α_3 as

$$\mathrm{disc}_{s_X} M_8 = 2i |M_5|^2 \frac{\beta_3(0) s_X^{\alpha_3 - 2\alpha_2} f(0, t_2, t_2)}{[\Gamma(-\alpha_2)\beta_{NPN}(t_2)]^2} . \tag{7.7}$$

In (7.7) $\beta_{NPN}(t_2)$ is the ordinary single-Regge proton-Pomeron-proton coupling. As we discussed in Sec. VI, (7.7) resembles the square of the amplitude for the exclusive reaction, modified by a "form factor" that depends on s_X and t_2. We remind the reader that this expression cannot be trivially obtained by extrapolating down to $s_X = m_N^2$, since as we mentioned in the discussion
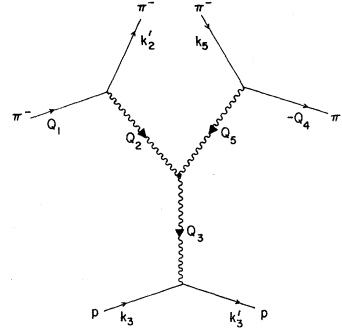

FIG. 17. Six-particle amplitude obtained by continuation to poles at $t_1 = m_\pi^2$ and $t_4 = m_\pi^2$.

following Eq. (2.6), the proton-pole contribution is singular.

Let us consider the contribution to M_8 from the trajectories at $\alpha_3 = \alpha_P$ and $\alpha_3 = \alpha_M$, where α_M is some effective meson trajectory with intercept $\frac{1}{2}$. These are shown in Fig. 17. The resultant contribution to (7.7) is given by

$$\mathrm{disc}_{s_X} M_8 = 2i |M_5|^2 \frac{[\beta_{NPN}(0) s_X^{1-2\alpha_2} f_{PPP}(0, t_2, t_2) + \beta_{NMN}(0) s_X^{1/2 - 2\alpha_2} f_{PPM}(0, t_2, t_2)]}{[\Gamma(-\alpha_2)\beta_{NPN}(t_2)]^2} . \tag{7.8}$$

The triple-Pomeron coupling[4] $f_{PPP}(0, t_2, t_2)$ and the Pomeron-Pomeron-meson coupling $f_{PPM}(0, t_2, t_2)$ are simply related to the inclusive distributions. As in Ref. 1, we take M_8 to be the helicity amplitude for which the ρ's have zero helicity in the t_1 and t_4 channel; the residue of our Reggeized form of M_5 at the pion pole is then given by

$$\mathrm{res} M_5 |_{t_1 = m_\pi^2} = -g_{\rho\pi\pi}(m_\rho^2 - 4m_\pi^2)^{1/2} \beta_{NPN}(t_2)\beta_{\pi P\pi}(t_2)\Gamma(-\alpha_2)\xi_2 s_2^{\alpha_2} . \tag{7.9}$$

From simple unitarity arguments, near $t_1 = m_\pi^2$ and $t_4 = m_\pi^2$, we have

$$M_8 \simeq \frac{(g_{\rho\pi\pi})^2 (m_\rho^2 - 4m_\pi^2) M_6}{(t_1 - m_\pi^2)(t_4 - m_\pi^2)} , \tag{7.10}$$

where M_6 is the six-particle amplitude shown in Fig. 17. The single-pion inclusive distribution for $\pi^- p \to \pi^- X$ is given by[2]

$$\frac{d\sigma_{\pi^- p \to \pi^- X}}{dq} = \frac{1}{2i\lambda^{1/2}(s_2, m_\pi^2, m_N^2)} \mathrm{disc}_{s_X} M_6 . \tag{7.11}$$

From (7.8)–(7.11), we may go to the pion poles in t_1 and t_4 and relate f_{PPP} and f_{PPM} to the single-pion inclusive distribution

$$\frac{d\sigma_{\pi^- p \to \pi^- X}}{dq} = [\beta_{\pi P\pi}(t_2)\xi_2]^2 \left[\left(\frac{s_X}{s_2}\right)^{1-2\alpha_2} \beta_{NPN}(0) f_{PPP}(0, t_2, t_2) + \left(\frac{s_X}{s_2}\right)^{1/2 - 2\alpha_2} \beta_{NMN}(0) \frac{f_{PPM}(0, t_2, t_2)}{\sqrt{s_2}} \right] . \tag{7.12}$$

We may now substitute (7.12) into (7.8) and obtain that

$$\mathrm{disc}_{s_X} M_8 = \frac{2i |M_5|^2 d\sigma_{\pi^- p \to \pi^- X}/dq}{16\pi s_2 d\sigma_{\pi^- p}^{el}/dt_2}$$

$$= \frac{2i |M_5|^2 d\sigma_{pp \to pX}/dq}{16\pi s_2 d\sigma_{pp}^{el}/dt_2} . \tag{7.13}$$

In the above, $d\sigma_{\pi^- p}^{el}/dt_2$ is the differential cross

section for $\pi^- p \to \pi^- p$. The second expression, which gives our result in terms of the inclusive distribution for $pp \to pX$ and the pp differential cross section, follows from the factorization of the single-Regge residues. We emphasize that (7.13) is only true when s_2 is sufficiently large so that the Pomeron dominates over the contributions from the other trajectories in the t_2 channel. Although (7.1) is a completely general multi-Regge

expression (7.13) will also be of direct importance to us due to the limited number of multi-Regge couplings that have been determined.

Now the distribution for the exclusive reaction $\pi^- p \to \rho^0 \pi^- p$ of Fig. 5 is given in terms of the quantities in (2.5) by

$$\frac{d\sigma^{ex}}{dM_{\rho\pi} dt_1 dt_2 d\phi_1} = \frac{1}{2^5 (2\pi)^4 \lambda(s_{12}, m_\pi^2, m_N^2)} \frac{|M_5|^2}{|\vec{p}_1^M|} .$$

(7.14)

If we substitute (7.13) into (2.6) and (2.7), we obtain the following result for the differential distribution of the inclusive reaction:

$$\frac{d\sigma}{dM_{\rho\pi} dt_1 dt_2 d\phi_1 ds_X} = \frac{d\sigma^{ex}}{dM_{\rho\pi} dt_1 dt_2 d\phi_1} V(s_X, t_2) ,$$

(7.15)

where

$$V(s_X, t_2) = \frac{d\sigma_{\pi^- p \to \pi^- X}/dq}{(4\pi)^2 s_2 d\sigma^{el}_{\pi^- p}/dt_2}$$

$$= \frac{d\sigma_{pp \to pX}/dq}{(4\pi)^2 s_2 d\sigma^{el}_{pp}/dt_2} .$$

(7.16)

When s_2 is large, $V(s_X, t_2)$ is independent of s_2. As we shall see, (7.15) and (7.16) provide a general relation that may be used to test the condition (5.37).

In order to calculate the amount of diffractive ρ-π production in the reaction of Fig. 1, we write the $\pi\rho$ total cross section as[26]

$$\sigma^{tot}_{\pi p} = \sigma^P_{\pi p} + \frac{\sigma^R_{\pi p}}{\sqrt{s_2}} ,$$

(7.17)

where $\sigma^P_{\pi p} = 21.3$ mb and $\sigma^R_{\pi p} = 19.7$ mb GeV. Then using the optical theorem, we may write[1]

$$\beta_{\pi P \pi}(t_2) \beta_{NPN}(t_2) = (\sigma^P_{\pi p}/\pi) e^{bt_2}$$

(7.18)

with $2b = 6.75$. As in Ref. 1, we take for the pion trajectory

$$\alpha_1 = -(m_\pi^2 - t_1)/(m_\pi^2 - t_1 + 1) ,$$

(7.19)

and for the Pomeron trajectory

$$\alpha_2 = 1.0 + 0.275 t_2 .$$

(7.20)

For the proton-proton elastic cross section, we write

$$\frac{d\sigma^{el}_{pp}}{dt_2} = \frac{(\sigma^{tot}_{pp})^2}{16\pi} e^{at_2} s_2^{2\alpha_2 - 2}$$

(7.21)

with $a = 6.84$ GeV^{-2}, $\sigma^{tot}_{pp} = 40$ mb.

For the inclusive proton distribution, we use the favored "solution 1" of Fox and Field. The Pomeron-induced contributions[26] are given by

$$s_2 \frac{d\sigma^P_{pp \to pX}}{dt_2 ds_X} = G_{PPP}(t_2) \left(\frac{\nu}{s_2}\right)^{1-2\alpha_P} + \frac{G_{PPM}(t_2)}{\sqrt{s_2}} \left(\frac{\nu}{s_2}\right)^{1/2 - 2\alpha_P} ,$$

(7.22)

where

$$G_{PPP}(t_2) = (2.32 e^{3.94 \, t_2} + 0.33 e^{1.12 \, t_2}) \text{ mb/GeV}^2 ,$$

(7.23)

$$G_{PPM}(t_2) = (0.95 e^{-0.01 \, t_2} + 3.45 e^{4.41 \, t_2}) \text{ mb/GeV}^2 ,$$

and

$$\nu = s_X - t_2 - m_N^2 .$$

In the above, the Pomeron trajectory is given by $\alpha_P = 1.0 + 0.36 \, t_2$, which is slightly different from the currently accepted (7.20).

At finite incident energy, in arbitrary regions of phase space, (7.8) will receive contributions from terms other than PPP and PPM. In the absence of any cuts on the data, this will have two effects. First, in order to calculate the inclusive distribution in (2.7), we must consider terms where either α_2 or α_5 is not the Pomeron trajectory; this is unfortunate since the fit to $pp \to pX$ that we shall use contains only diagonal terms, and in addition, we must deduce other double-Regge couplings besides (2.13) and (2.14). Second, the factorization condition (7.15) will break down. Since (7.15) is a useful test of the identity of the double-Regge couplings in the multi-Regge and the HPRP limit, we would like to perform cuts on the data to guarantee that only the PPP and PPM terms contribute.

With the above goals in mind, we shall have the following plan of attack. First, we will calculate the inclusive distribution using (7.15)–(7.23), so that the diffractive contribution from PPP and PPM is known. Second, we will estimate the contribution from nondiffractive production, and then perform kinematic cuts on our result in order to isolate a region of phase space where these nondiffractive effects are negligible. Finally, having isolated such a region, we shall compare (7.15) with real data and check for agreement.

In order to estimate the total ρ-π production, diffractive plus nondiffractive, we can recalculate the mass spectrum, replacing (7.18) with

$$\beta_{\pi P \pi}(t_2) \beta_{NPN}(t_2) = \frac{\sigma^{tot}_{\pi p}}{\pi} e^{bt_2} ,$$

where $\sigma^{tot}_{\pi p}$ is given by (7.17). (This procedure is for estimation purposes. We will ultimately try to minimize the nondiffractive effects that we have inserted in a "non-Regge" fashion.) For the inclusive $pp \to pX$ distribution, we include the MMP and MMM terms of Fox and Field[26] (note that π exchange does not contribute due to G-parity requirements). From their solution 1, the nondiffractive contribution is

$$s_2 \frac{d\sigma^M_{pp \to pX}}{dt_2 ds_X} = G_{MMP}(t_2)\left(\frac{\nu}{s_2}\right)^{1-2\alpha_M}$$

$$+ \frac{G_{MMM}(t_2)}{\sqrt{s_2}}\left(\frac{\nu}{s_2}\right)^{1/2 - 2\alpha_M}, \qquad (7.24)$$

where

$$G_{MMP}(t_2) = (26.81\ e^{7.26\ t_2} + 4.80 e^{-1.83\ t_2})\ \text{mb/GeV}^2,$$

$$G_{MMM}(t_2) = (18.1 e^{12.0\ t_2})\ \text{mb/GeV}^2,$$

$$\alpha_M = 0.5 + t_2.$$

In Fig. 18, we show the results of some pre-liminary calculations, using an incident pion with laboratory momentum 147 GeV/c. Using a simple Monte Carlo program, we calculated a sample of events in the missing-mass interval $4 \leqslant s_X \leqslant 25$ GeV^2, and ρ-pion mass interval $0.95 \leqslant M_{\rho\pi} \leqslant 1.50$ GeV. As in Ref. 1, we demand that $|t_1| \leqslant 2.5$ GeV^2 and $|t_2| \leqslant 1.0$ GeV^2. In Fig. 18, curve A shows our estimate to total ρ-π production. Curve B shows our calculation of the diffractive ρ-π production. We remind the reader that in comparing with real data on $\pi^- p \to \pi^- \pi^+ \pi^- X$, one should multiply our results by a "standard" factor[1,27] of about 2. This is due to the fact that the ρ does not fill up all $\pi^+\pi^-$ partial waves. As we can see, the pure dif-fractive contribution is about $\frac{1}{3}$ the total cross sec-tion in this kinematic region.

Since we have the expressions (2.14) and (2.15), we would like to isolate the kinematic region where the cross section is dominated by the diffractive contribution (i.e., Pomeron exchange). It is in-structive to look at Fig. 19, where we see the dis-tribution in missing mass squared, s_X. Again, curve A is our estimate to the total ρ-π production, and curve B is our calculation of the diffractive contribution. We see that the diffractive contribu-tion dominates in the region where s_X is small,
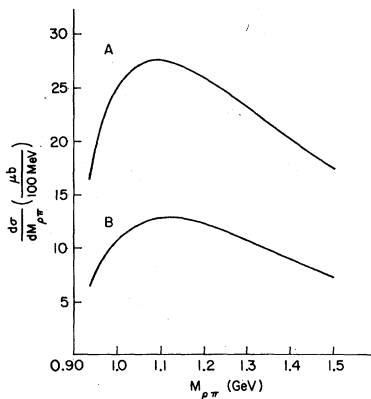

FIG. 18. Calculated ρ-π mass distributions for P_{lab} = 147 GeV/c; curve A, estimated total ρ-π production; curve B, diffractive ρ-π production. $4 \leqslant s_X \leqslant 25$ GeV^2 for both curves.
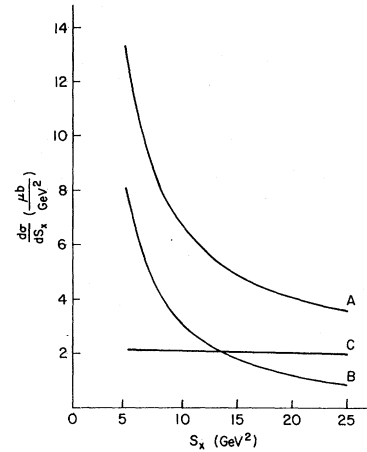

FIG. 19. Distribution in missing mass squared, s_X; curve A, estimated total; curve B, diffractive contribu-tion; curve C, largest nondiffractive contribution from MMM term.

as one may verify by comparing (7.23) and (7.24). The largest nondiffractive contribution comes from the MMP term, and is given by curve C in Fig. 19. We see that it produces a flat distribution in s_X and dominates for large s_X. If we recall that from (3.36) and (4.12), we have $|e^{iX_B}| = |e^{iX_E}| \sim s_2/s_X$ in the HPRP limit, we see that our approach to the HPRP limit is governed by the value of this ratio,[28] rather than the individual values of s_X and s_2 (as-suming that both are sufficiently large so as to be out of the resonance region). As a result, if we select only those events in which the ratio s_2/s_X is large, we isolate both the HPRP limit of M_8 and the diffractive contribution. Since the diffractive contribution continues to rise as s_X becomes small, if we also consider inclusive events where $s_X < 4$ GeV^2, the diffractive contribution to the cross sec-tion should be proportionately larger, even though the multi-Regge expansion appears to break down[26] for $s_X < 2$ GeV^2 [in this region, our expression for M_5 remains valid, but our expression for $V(s_X, t_2)$ breaks down].

In Fig. 20, we see the resulting ρ-π mass spec-trum that results when we keep only those events in our original sample satisfying $s_2/s_X \geqslant 8$. We see that the relative fraction of diffractive events has increased markedly; as before, we expect that the relative contribution of the diffractive events can be further increased by including those events with $s_X \leqslant 4$ GeV.^{2} In Fig. 21, we show the missing-mass distribution for events satisfying our cut; we see that we have suppressed the nondiffractive contributions at all values of s_X.

Let us now apply the preceding formalism to $\pi^- p \to \pi^- \pi^+ \pi^- X$. Let the four-momenta of the final-state pions $\pi^- \pi^+ \pi^-$ be q_-, q_+, q. We can consider
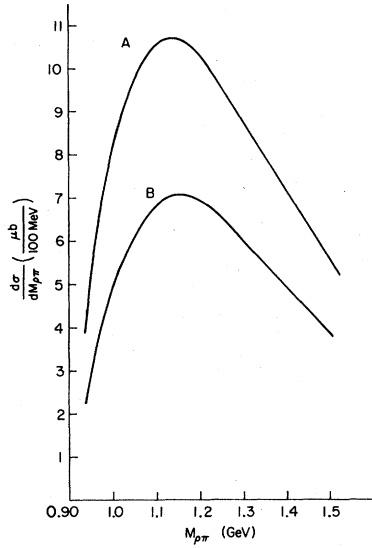
FIG. 20. Calculated ρ-π mass distributions as in Fig. 18, subject to the cut $s_2/s_x \geq 8$; curve A, estimated total ρ-π production; curve B, diffractive contribution.

the amplitude to be due to diagrams such as those in Fig. 22, where a dipion is produced by ρ decay (for dipion masses away from the ρ mass, one expects that the interaction at the upper vertices can be approximated by π-π scattering). Then the inclusive cross section can be expressed in terms of diagrams like those shown in Fig. 23, where we perform all possible interchanges of the final-state pions on the left side of the diagram, and of the initial-state pions on the right side of the diagram.

If we let the four-momentum of the dipion be $q_1 = q_+ + q_-$, the kinematic quantities in (2.5) are
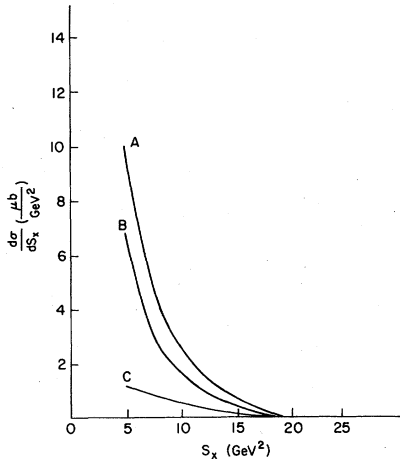
FIG. 21. Distribution in s_x, for $s_2/s_x \geq 8$; curve A, estimated total; curve B, diffractive contribution; curve C, estimated MMM contribution.
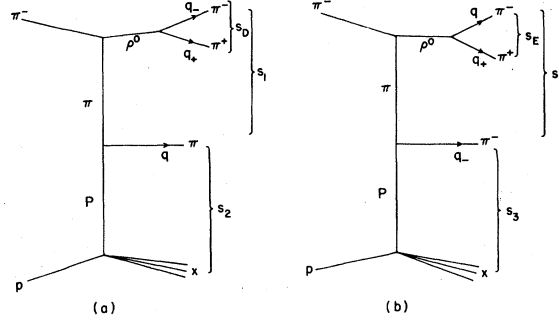

FIG. 22. Diagrams contributing to $\pi^- p \to \pi^- \pi^+ \pi^- X$ through ρ decay.

unchanged, except for the replacement $m_\rho^2 \to s_D$, where $s_D = (q_+ + q_-)^2$. We can further specify the physical-region kinematics by defining the D frame, in which

$$\vec{q}_1^D = \vec{q}_+^D + \vec{q}_-^D = 0 \,,$$

$$p_1^D = (p_{10}^D, 0, 0, |\vec{p}_1^D|) \,,$$

$$q^D = (q_0^D, |\vec{q}^D| \sin\psi_D, 0, |\vec{q}^D| \cos\psi_D) \,,$$ (7.25)

$$q_-^D = (q_{-0}^D, |\vec{q}_-^D| \sin\theta_D \cos\phi_D, $$

$$|\vec{q}_-^D| \sin\theta_D \sin\phi_D, |\vec{q}_-^D| \cos\theta_D) \,.$$

The orientations of the momenta in the D frame are shown in Fig. 24. The quantities in the D frame are given by

$$p_{10}^D = \frac{s_D + m_\pi^2 - t_1}{2\sqrt{s_D}}, \quad |\vec{p}_1^D| = [(p_{10}^D)^2 - m_\pi^2]^{1/2} \,,$$

$$q_0^D = \frac{s_1 - s_D - m_\pi^2}{2\sqrt{s_D}}, \quad |\vec{q}^D| = [(q_0^D)^2 - m_\pi^2]^{1/2} \,,$$

$$q_{-0}^D = q_{+0}^D = \frac{\sqrt{s_D}}{2}, \quad |\vec{q}_-^D| = |\vec{q}_+^D| = [(q_{-0}^D)^2 - m_\pi^2]^{1/2}, \quad (7.26)$$

$$\cos\psi_D = \frac{2q_0^D p_{10}^D + s_D - s_1 + t_2 - t_1}{2|\vec{q}^D||\vec{p}_1^D|} \,,$$

$$\sin\psi_D = (1 - \cos^2\psi_D)^{1/2} \,,$$

$$M_{3\pi} = \sqrt{s_1}, \quad M_{2\pi} = \sqrt{s_D},$$
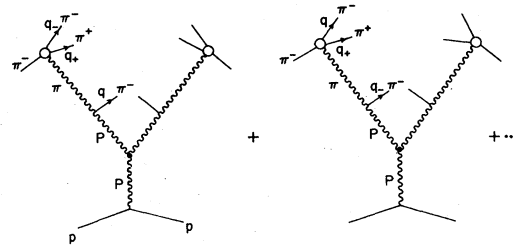
$$s_3 = (q_- + Q_X)^2, \quad s_4 = (q_+ + Q_X)^2 \,.$$

FIG. 23. Typical ten-particle amplitudes contributing to inclusive 3π production. Upper blobs correspond to π-π scattering.
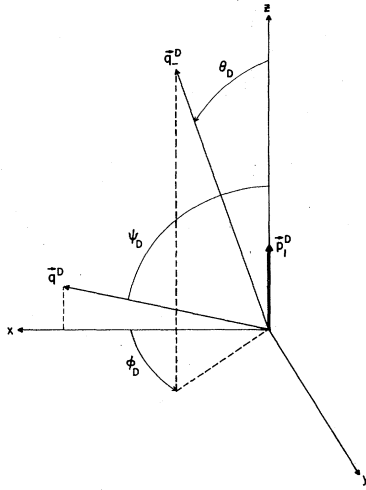
FIG. 24. Orientation of vectors in the D frame ($\pi^+\pi^-$ rest frame).

Then in exactly the same fashion as we obtained (7.15), we have the following relation between the inclusive and exclusive distributions:

$$\frac{d\sigma}{dM_{3\pi}dM_{2\pi}d\Omega_D dt_1 dt_2 d\phi_1 ds_X} = \frac{d\sigma^{ex}}{dM_{3\pi}dM_{2\pi}d\Omega_D dt_1 dt_2 d\phi_1}$$
$$\times V(s_X, t_2), \qquad (7.27)$$

where $d\Omega_D = d(\cos\theta_D)d\phi_D$, and $V(s_X, t_2)$ is given by (7.16). We point out that in order to isolate the PPP and PPM terms at the triple-Regge vertex, we must also demand that s_3/s_X and s_4/s_X be large. At finite incident pion energy, we must impose the condition that

$$\frac{s_2}{s_X}, \frac{s_3}{s_X}, \frac{s_4}{s_X} \geq R, \qquad (7.28)$$

where R is some large number (say 5 or 8). This last condition not only isolates the Pomeron contributions to all of the diagrams in Fig. 19, but it also guarantees that those diagrams are in the HPRP limit. In addition, (7.28) ensures that it does not make any difference whether we use s_2, s_3, or s_4 in evaluating the cross sections appearing in (7.16). In addition, we should use only the diffractive contribution to the inclusive pp cross section given by the fits[26] (7.22) and (7.23).

In order to appreciate the significance of (7.27) let us state the necessary assumptions for its validity.

(1) The amplitude is evaluated in the HPRP limit. This is guaranteed by imposing (7.28).

(2) The amplitude receives its main contribution from a particular trajectory where $\alpha_2 = \alpha_5$. This may be satisfied for an arbitrary reaction by the quantum numbers of the allowed exchanges; in the case of the Pomeron trajectory, this is automatic-

ally achieved by imposing (7.28).

(3) Conditions such as (5.39) hold, so that the double-Regge couplings are identical to those in the exclusive case.

Note that condition (2) contains the implicit assumption that the amplitude is dominated by Regge poles (at least in α_2 and α_5); this appears to be the case for the exclusive reaction $\pi^- p \to \pi^-\pi^+\pi^- p$.[1,25,27] The first two assumptions are guaranteed by our kinematic cuts; assumption (3) must be verified experimentally.

If we attempt to compare our results with reported data,[29] for $\pi^- p \to \pi^-\pi^+\pi^- X$ at $p_{lab} = 147$ GeV/c (Fermilab experiment E154), we find that a detailed comparison with experiment is difficult, since the cuts made on the data were somewhat different from ours. Since the missing-mass distribution goes like $1/s_X$, the calculated cross section is extremely sensitive to the lower bound on this cut. In addition, due to the usual problems with finite missing-mass resolution, the $1/s_X$ dependence of the diffractive contribution makes it somewhat difficult to determine accurately the magnitude of this contribution at low missing mass.

In spite of these difficulties, there are several features of the data that suggest that our analysis is correct. We shall briefly describe their analysis of the data, which came from an initial sample of 105 000 $\pi^- p$ pictures in the Fermilab proportional hybrid system. The data that were analyzed consisted of only those events which have survived a particular cut in the pion rapidity y. The cut was made, in effect, by first measuring the rapidities of all charged tracks in each bubble-chamber picture, ordering the tracks so that the first track had the largest rapidity, the second track had the next largest, etc. Only those events were kept in which the gap in rapidity between the third and fourth track, Δy, was greater than the average rapidity gap between all tracks in that event. The final criterion was that the three leading tracks had a net total charge of -1.

We see that the net effect of the above cuts is to group the observed pions together in rapidity space. This is similar to, but not identical with, the effect of (7.28). This similarity may be seen by considering the Feynman variable x, where $x = 2p_{\parallel}/\sqrt{s_{12}}$. Let x_+, x_-, and x correspond to q_+, q_-, and q in the overall center of mass. Then if s_1 is small compared to s_2, s_{12}, and s_X, and if we take the pions to be produced mainly in the longitudinal direction,

$$s_2 = s_{12}(1 - x_+ - x_-),$$
$$s_3 = s_{12}(1 - x_+ - x), \qquad (7.29)$$
$$s_4 = (1 - x_- - x),$$

$$s_X = s_{12}(1 - x_+ - x_- - x) = S_2 - x s_{12}$$

$$= s_3 - x_- s_{12} = s_4 - x_+ s_{12}. \qquad (7.30)$$

Then $s_2/s_X \geq R$ implies

$$x \geq (R - 1)(1 - x_+ - x_-)/R$$

and similarly,

$$x_+ \geq (R - 1)(1 - x - x_-)/R,$$

$$x_- \geq (R - 1)(1 - x_+ - x)/R. \qquad (7.31)$$

If we impose a lower cutoff on the missing mass $s_{X\,\mathrm{min}}$ so that we are above the resonance region, we have

$$x_+ + x_- + x \leq 1 - s_{X\mathrm{min}}/s_{12}. \qquad (7.32)$$

It is easy to see that (7.31) and (7.32) tend to group the particles together with $x_+ \simeq x_- \simeq x$. Hence, the condition (7.28) is similar to (but not identical with) the rapidity-gap analysis reported in Ref. 29.

There are several features of the data that suggest that our analysis is relevant in the region (7.29). First of all, after the rapidity-gap analysis is performed on the data,[29] one sees a clear ρ signal in the $\pi^+\pi^-$ mass spectrum only after the additional cut $s_X \leq 25$ GeV^2 is made. This tends to select the region (7.28), and also suggests pion exchange in the t_1, t_4 channels (and those channels obtained by permuting the final-state pions). Another encouraging feature of the data is that the calculated diffractive mass spectrum in Fig. 20 (times a standard factor of 2) is roughly the same size and shape. Owing to the different nature of the cuts (and of course, experimental uncertainties) we find this agreement encouraging. One final bit of supportive evidence reported[29] is that

$$\sigma_{\pi^-p \to \pi^-\pi^-\pi^+\pi^-X} \simeq \frac{\sigma_{\pi^-p \to \pi^-\pi^+\pi^-p}\sigma_{\pi^-p \to \pi^-X}}{\sigma^{el}_{\pi^-p}}. \qquad (7.33)$$

The above appears to be approximately valid only for $s_X < 25$ GeV^2. This is clearly consistent with the validity of the detailed relation (7.27) in the region (7.28).

From the preceding discussion, it seems that the most sensitive test of the identity of the double-Regge couplings in the inclusive and exclusive reactions is to integrate both sides of (7.27) over a missing-mass range, say 4 GeV^2 $\leq s_X \leq 25$ GeV^2 (assuming $p_{\mathrm{lab}} = 25$ GeV/c), and compare the resulting angular distributions. Although the overall normalization should agree, they are unfortunately quite sensitive to the lower cut on s_X, due to the $1/s_X$ dependence.

VIII. DISCUSSION

In light of the preceding discussion, it appears that a high-statistics study of $\pi^-p \to \pi^-\pi^+\pi^-X$ in the "Deck region" of Sec. II should prove quite inter-

esting. If one finds detailed agreement between the angular distributions in the inclusive and exclusive reactions so that (7.27) is satisfied in the region given by (7.28), then we will have experimental support for the identity of the multi-Regge vertices in the inclusive and exclusive reactions. On the other hand, if one can show that (7.27) is clearly false, then the "Deck background"[1,25,27] in the 3π mass spectrum for the inclusive case must be different from the background in the exclusive case. In this case, one would hope that the presence of an A_1 resonance could be observed.

We also should mention that the ideas that we have discussed might be investigated much better in other reactions. This may be seen by considering the effect of (7.28) in the 3π center of mass (M frame). From (2.5), s_2 is given by the expression

$$s_2 = s_X + m_\pi^2 + 2q_0^M Q_{X0}^M$$

$$+ 2|\vec{q}^M||\vec{Q}_X^M|(\cos\theta_1\cos\psi_2 + \sin\theta_1\sin\psi_2\cos\phi_2). \qquad (8.1)$$

If s_{12}/s_1 is large, then

$$s_2 \simeq s_X + m_\pi^2 + \frac{s_{12}}{\sqrt{s_1}}[q_0^M + |\vec{q}^M|(\cos\theta_1\cos\psi_2 + \sin\theta_1\sin\psi_2\cos\phi_1)]. \qquad (8.2)$$

Similar expressions result from considering s_3 and s_4. The effect of (7.28) at fixed center-of-mass energy is to limit the angular region over which (7.27) holds. It may turn out that pp or $p\bar{p}$ colliding-beam experiments may provide a better test of relations such as (7.27) in other reactions.

If (7.27) appears to be valid, it is interesting to speculate on other experiments where the A_1 might be produced by strong interactions. We remind the reader that in the exclusive reaction $\pi^-p \to \pi^-\pi^+\pi^-p$, one is searching for an A_1 pole term corresponding to a diagram like the one in Fig. 25. The fact that such a term is not present in the data in an obvious fashion is due, at least in part,
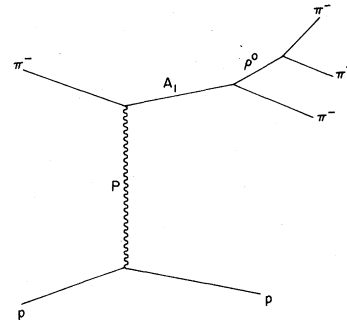

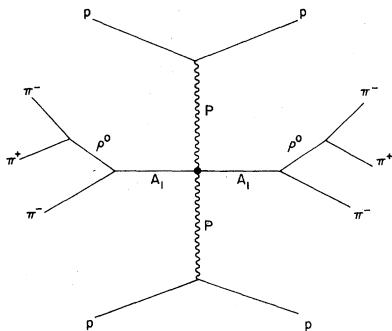FIG. 25. Pole term corresponding to the A_1 thought to be present in $\pi^-p \to \pi^-\pi^+\pi^-p$.

FIG. 26. Double-pole term that may be present in pp $\rightarrow \pi^-\pi^+\pi X$.

to the nonresonant background.[1] Since the amplitude for the inclusive reaction in the HPRP limit is nearly identical to that for the five-particle amplitude [assuming (5.39) is true], it seems unlikely that the "true A_1 resonance" will be seen in the kinematic region (7.28) either. An interesting candidate, however, is the reaction $p\bar{p}\rightarrow \pi^-\pi^+\pi^-X$. If we look at 3π combinations where the 3π system has a net rapidity near zero, it may be possible to isolate diagrams such as those in Fig. 26. In order to be sure that we are in a kinematic region where the expansion of Fig. 26 is appropriate, the rapidity distribution of 3π events at fixed $M_{3\pi}$ must exhibit a flat central plateau, just as the single-pion inclusive distribution. Since we are concerned with three-pion mass combinations with $M_{3\pi}\gg m_\pi$, the amount of rapidity space available to the 3π system is considerably less than that available to the individual pions; due to energy requirements, it seems that we must, for the present, consider either pp or $p\bar{p}$ colliding beams. Now if one can establish that such a plateau exists, then if $Y_{3\pi}$ is the rapidity of the $\pi^-\pi^+\pi^-$ system, we expect that $d\sigma/dM_{3\pi}|_{Y_{3\pi}=0}$, after phase-space corrections, should exhibit a sharp rise near the A_2 mass, and (we hope) a similar rise will occur near the real A_1. Clearly processes other than those shown in Fig. 26 will contribute to the inclusive cross section; however, regardless of their size, one naively expects that their effect should be systematically different from the usual Deck effect.

IX. SUMMARY

In closing, let us attempt to summarize our results. We showed that owing to the relatively small size of the term H_2 in $\pi^-p\rightarrow \rho^0\pi^-p$, we expect that a multi-Regge analysis of $\pi^-p\rightarrow \rho^0\pi^-X$ should work in the region of low ρ-π mass. We showed that as we approach the kinematic limit necessary for the application of Mueller's optical theorem, the MFD, the SO(2, 1) group parameters

for the expansion of M_8 correspond precisely to those describing a "naive" amplitude where we treat the missing-mass four-momentum as belonging to a quasiparticle. We extended previous analysis of the six-particle amplitude to the eight-particle case, and analytically continued the SO(2, 1) parametrization into an O(3) parametrization. We were thus able to show that certain polar and azimuthal angles become large in the limit of interest, and that the amplitude is therefore dominated by a mixture of Regge poles and helicity poles.

We refined previous notions of the nature of helicity poles by showing that the azimuthal angles that give rise to the helicity-pole behavior become identical with the polar angles for our "naive" momentum set as we approach the "forward direction" [actually, the manifold R given by (6.13)]. Our particular group-theoretic limit is distinguished in this respect from other limits that give the same asymptotic limit of the invariant subenergies, but give limiting forms of M_8 that do not have discontinuities in s_X (and hence do not contribute to the inclusive cross section). In these other group-theoretic limits, the azimuthal angles do not transform into polar angles, and hence the full parametrization does not reduce to a "naive" one.

We also showed that due to the locations of the complex helicity contours, the double-Regge vertices are the same for the inclusive and exclusive reactions if the Regge residues have a general type of smooth behavior in the auxiliary variables. Our improvement in the understanding of this problem is twofold. First, due to the location of the helicity contours, the identity of the vertices will result from the residues being independent of Φ_2 and Φ_5 [see (5.39)]. Second, our kinematic study of the azimuthal angles at the triple-Regge vertex suggests that such behavior must be present.

In a straightforward manner, we have obtained a multi-Regge amplitude for $\pi^-p\rightarrow \rho^0\pi^-X$, where the amplitude is fixed in terms of previously determined single-, double-, and triple-Regge residues. We were then able to estimate the ratio of diffractive to nondiffractive production of ρ-π systems. We showed that the region where diffractive production is largest coincides with the region where our expansion is valid. We demonstrated that our analysis is qualitatively similar to the standard rapidity-gap analysis, but that the Feynman variable x is more appropriate that rapidity. Our prediction of the diffractive contribution agrees with the data, which unfortunately suffer from low statistics.

Lastly, we have proposed experimental tests to verify the identity of the double-Regge couplings for the inclusive and exclusive reactions, given by

(7.15) and (7.16). We predict detailed relations between the two reactions over well-defined kinematic regions. These relations, which may be extended to other reactions, predict similar angular distributions for the ρ-π system in the previously mentioned kinematic region. A violation of these relations may suggest an exciting region in which to search for the A_1.

ACKNOWLEDGMENTS

[1]M. J. Puhala, Phys. Rev. D **17**, 814 (1978); **18**, 4358 (E) (1978).

[2]C. E. DeTar, D. Z. Freedman, and G. Veneziano, Phys. Rev. D **4**, 906 (1971).

[3]A. H. Mueller, Phys. Rev. D **2**, 2963 (1970); C. E. DeTar *et al.*, Phys. Rev. Lett. **26**, 675 (1971).

[4]R. C. Brower, C. E. DeTar, and J. H. Weis, Phys. Rep. **14C**, 259 (1974).

[5]J. H. Weis, Phys. Rev. D **6**, 2823 (1972).

[6]H. D. I. Abarbanel and A. Schwimmer, Phys. Rev. D **6**, 3018 (1972).

[7]M. Toller, Nuovo Cimento **37**, 631 (1965).

[8]M. N. Misheloff, Phys. Rev. **184**, 1732 (1969).

[9]N. F. Bali, G. F. Chew, and A. Pignotti, Phys. Rev. **163**, 1572 (1967).

[10]I. O. Moen and W. J. Zakrezewski, Nucl. Phys. **B65**, 346 (1973).

[11]O. Steinmann, Helv. Phys. Acta. **33**, 275 (1960); **33**, 347 (1960).

[12]H. P. Stapp, Phys. Rev. D **3**, 3177 (1971).

[13]R. J. Eden, P. Landshoff, D. Olive, and J. Polkinghorne, *The Analytic S-Matrix* (Cambridge University Press, Cambridge, England, 1966).

[14]Chan Hong-Mo, K. Kajantie, and G. Ranft, Nuovo Cimento **49A**, 157 (1967).

[15]J. F. Boyce, J. Math. Phys. **8**, 675 (1967).

[16]C. E. Jones, F. E. Low, and J. E. Young, Ann. Phys. (N.Y.) **63**, 476 (1971).

[17]C. E. Jones, F. E. Low, and J. E. Young, Ann. Phys. (N.Y.) **70**, 286 (1972).

[18]J. H. Weis, Phys. Rev. D **5**, 1043 (1972).

[19]A. R. White, Nucl. Phys. **B39**, 432 (1972).

[20]C. E. DeTar and J. H. Weis, Phys. Rev. D **4**, 3141 (1972).

[21]J. H. Weis, Phys. Lett. **43B**, 487 (1973).

[22]C. E. Jones, F. E. Low, and J. E. Young, Phys. Rev. D **6**, 640 (1973).

[23]I. T. Drummond, P. V. Landshoff, and W. J. Zakrezewski, Phys. Lett. **28B**, 676 (1969).

[24]J. C. Polkinghorne, Nuovo Cimento **7A**, 555 (1972).

[25]G. Ascoli *et al.*, Phys. Rev. D **9**, 1963 (1974).

[26]R. D. Field and G. C. Fox, Nucl. Phys. **B80**, 367 (1974).

[27]E. L. Berger, Phys. Rev. **166**, 1525 (1968).

[28]R. G. Roberts, in *Phenomenology of Particles at High Energies*, edited by R. L. Crawford and R. Jennings (Academic Press, New York, 1974).

[29]J. W. Cooper *et al.*, talk EK10 presented at Washington APS meeting, 1977 (unpublished).